EARTH SURFACE PROCESSES AND LANDFORMS
Earth Surf. Process. Landforms (2010)

Published online in Wiley InterScience
(www.interscience.wiley.com) DOI: 10.1002/esp.2023

Controls on at-a-station hydraulic geometry in steep headwater streams, Colorado, USA

Gabrielle C. L. David,[1]* Ellen Wohl,[1] Steven E. Yochum[2] and Brian P. Bledsoe[2]
[1] Department of Geosciences, Colorado State University, Fort Collins, CO, USA
[2] Department of Civil and Environmental Engineering, Colorado State University, Fort Collins, CO, USA

Received 5 October 2009; Revised 21 February 2010; Accepted 1 March 2010

*Correspondence to: Gabrielle C. L. David, Department of Geosciences, Colorado State University, Fort Collins, CO 80523, USA. E-mail: gcldavid@warnercnr.colostate.edu

ESPL
Earth Surface Processes and Landforms

ABSTRACT: Detailed hydraulic measurements were made in nine step-pool, five cascade and one plane-bed reach in Fraser Experimental Forest, Colorado to better understand at-a-station hydraulic geometry (AHG) relations in these channel types. Average values for AHG exponents, m (0·49), f (0·39), and b (0·16), were well within the range found by other researchers working in steep gradient channels. A principal component analysis (PCA) was used to compare the combined variations in all three exponents against five potential control variables: wood, D_{84}, grain-size distribution (σ), coefficient of variation of pool volume, average roughness-area (projected wetted area) and bed gradient. The gradient and average roughness-area were found to be significantly related to the PCA axis scores, indicating that both driving and resisting forces influence the rates of change of velocity, depth and width with discharge. Further analysis of the exponents showed that reaches with $m > b + f$ are most likely dominated by grain resistance and reaches below this value ($m < b + f$) are dominated by form resistance. Copyright © 2010 John Wiley & Sons, Ltd.

KEYWORDS: at-a-station hydraulic geometry (AHG); hydraulic measurements; principal component analysis (PCA); channels

At-a-station Hydraulic Geometry and Flow Resistance

At-a-station hydraulic geometry (AHG) characterizes how changes in discharge affect specific hydraulic variables such as width, depth, velocity and friction. Leopold and Maddock (1953) first coined the term 'hydraulic geometry' to describe systematic changes both downstream and at a cross-section for each of the above hydraulic variables. They proposed three power relations to describe how width ($w = aQ^b$), depth ($d = cQ^f$) and velocity ($v = kQ^m$) vary with discharge both downstream and at a given cross-section in a channel, where Q is discharge; w is water-surface width, d is mean depth; and v is velocity. These power relations are bound by the continuity equation ($Q = wdv$), so that the coefficients a, c, and k have a product equal to one and the exponents b, f, and m sum to one. Leopold and Maddock (1953) found that the rates of change of width, depth and velocity with discharge were related to the shape of the channel, the slope of the water-surface and the roughness of the wetted perimeter. They also found the sediment load to be an important control on the rates of change of both velocity and depth (Leopold and Maddock, 1953).

Few studies have reported AHG values for steep mountain channels (Lee and Ferguson, 2002; Reid, 2005; Comiti *et al.*, 2007). A better understanding of at-a-station changes in each of the above hydraulic variables can improve our understanding of the sources and magnitude of hydraulic roughness in these channels, which tend to have values of flow resistance as reflected in Manning's n or Darcy–Weisbach friction factor (ff) that are much higher than values for channel reaches with gradient <1% (Jarrett, 1984; Bathurst, 1985, 1993).

Steep mountain channels are divided into cascade, step-pool and plane-bed channel morphologies (Grant *et al.*, 1990; Montgomery and Buffington, 1997). Cascade morphologies are characterized by tumbling flow over individual randomly arranged clasts and form at $S_0 > 0{\cdot}06$ (where S_0 is bed gradient). Step-pools have a consistent step and pool morphology ($0{\cdot}03 < S_0 < 0{\cdot}10$) and plane-bed ($0{\cdot}01 < S_0 < 0{\cdot}03$) have no distinctive variations in the bed (Montgomery and Buffington, 1997). Many at-a-station studies have focused on lower gradient pool-riffle channels, which have significantly different hydraulic relations between pools and riffles (Richards, 1976). Few studies have focused specifically on differences between cascade, step-pool and plane-bed reaches, which might be expected to exhibit differences in at-a-station relations because of the differences in channel configuration and primary source of roughness.

Subsequent investigators have confirmed that cross-sectional shape and flow resistance are significant in determining how width and velocity vary with depth (Knighton, 1974, 1975; Richards, 1976; Ferguson, 1986; Ridenour and Giardino, 1995; Wohl, 2007). Ferguson (1986) showed that depth would

increase faster than width in a rectangular channel, but in a more triangular channel width may increase faster than depth. The variation in velocity with depth is related to frictional characteristics. In a channel where increasing flow depth quickly drowns out the effects of roughness elements, velocity would increase quickly with depth. Knighton (1975) proposed that a channel dominated by grain resistance would have the highest rates of decrease in resistance as discharge increases.

Park (1977) found that a wide range of the three hydraulic geometry exponents exists throughout the world, which suggests the need for an improved understanding of the sources of variation. Other controls on at-a-station values that have been identified include differences between braided, meandering, and straight reaches (Knighton, 1975; Ferguson, 1986); differences based on bank composition (Knighton, 1974); variations between pool and riffle sections (Knighton, 1975; Richards, 1976); and differences based on irregularities in resistance in relation to stage (Richards, 1976; Ferguson, 1986). Ferguson (1986) also noted that AHG may vary over the course of a flood cycle as both scour and fill occur during this time period. The effect of the flood cycle on AHG may be particularly important in higher gradient streams where the beds are armored and the channel form is thought to have developed during large events (Grant *et al.*, 1990; Church and Zimmerman, 2007).

The use of power relations in hydraulic geometry analysis is a mathematical convenience that lacks a theoretical foundation (Park, 1977; Richards, 1973; Ferguson, 1986). Other statistical models have been proposed for representing AHG including Richards' (1973) log-quadratic model and Bates' (1990) piecewise linear regression approach, but neither of these are as widely used as the power law relations. Unfortunately, statistical models are limited by the range of data used and cannot typically be extended outside that range. Despite these drawbacks, these models can be used to further understand differences in AHG values and to find previously unrecognized relationships between variables (Rhoads, 1992).

Width, depth, velocity, discharge, flow resistance and sediment transport capacity are all interrelated. The number of variables that mutually adjust is greater than the number of equations available to describe these adjustments (Ferguson, 1986, Phillips, 1990). Further work has been done using extremal hypotheses to develop a theoretical framework for predicting AHG values and to better describe these adjustments (Langbein, 1964; Huang and Nanson, 2000; Singh and Zhang, 2008a). Although these extremal hypotheses are important in the attempts to predict AHG, the objective of this paper is to describe and understand differences in AHG among reaches rather than to predict the actual values, and consequently to improve our understanding of how a system adjusts to disturbances (Phillips, 1990).

The relationship between resistance and stage (ff = oQ^x) is also important in understanding how width, depth and velocity vary with stage. Leopold *et al.* (1960) showed that resistance may not vary continuously with discharge. Knighton (1974) and Richards (1976) suggest that the sources of resistance vary in an irregular cross-section as point bars and island deposits are inundated with increasing discharge. Others have reported inflection points in data: as flow increases and water begins to spill over bars (Hogan and Church, 1989); where the bed begins to mobilize (Knighton, 1998; Hickin, 1995); and when larger grains are submerged, decreasing flow resistance (Knighton, 1998; Bathurst, 1982). Wohl (2007) found a decreased rate of change in velocity and water-surface gradient at higher discharges in a pool-riffle channel and surmised that the inflection point reflected a transition from decreasing grain roughness to increasing form roughness. Therefore, resistance does not necessarily vary as a power relationship with discharge.

Sources of resistance in step-pool and cascade reaches include wood, individual grains, and the channel form. Resistance in these channels is most often subdivided into spill, form and grain resistance (Ferguson, 2007; Wilcox and Wohl, 2006). Spill resistance is created from sharp flow transitions as flow plunges over steps or from wave drag over elements protruding above the water-surface. Grain resistance is from skin friction and form drag around individual grains and form resistance is created from dunes, steps and bars in the channel (Wilcox and Wohl, 2006). Each of these types of resistance varies as discharge varies in a reach. At higher flows, protruding grains occupy a smaller proportion of the total flow depth and form resistance may become the dominant type of resistance. Spill resistance is significant at both low flows, when the step heights are the largest, and high flows, when larger waves cause greater energy dissipation (Comiti *et al.*, 2007; Church and Zimmerman, 2007). Resistance associated with wood can be both from grain resistance around individual logs and form resistance around larger log jams and steps. Wood in the channels may also be inundated at different flow levels, causing the amount of resistance associated with the wood to vary with discharge. Therefore, the rate of change of resistance depends on the water depth and the different forms of resistance at that cross-section (Knighton, 1975). Changes in width, depth and velocity at a section are intertwined with these variations in resistance; therefore, examining AHG is essential to understanding the interactions between all five variables [wood load, sediment size, pool size, gradient, roughness-area (Figure 1 and Table I)] and flow.

Ridenour and Giardino (1991) proposed that because hydraulic geometry data are unit-sum constrained they should be analyzed as a composition in order to understand how

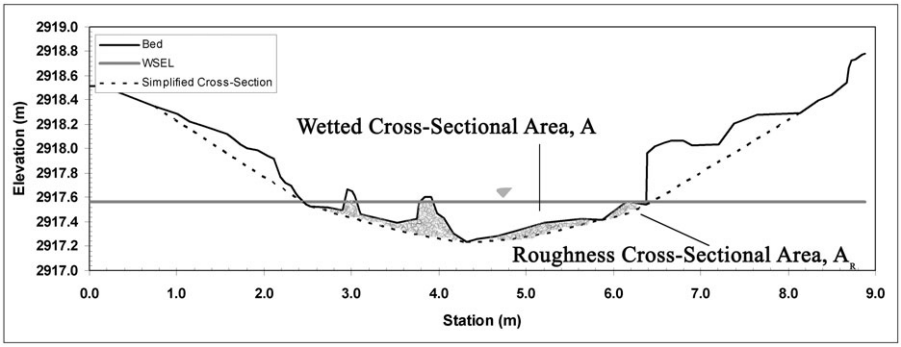

Figure 1. Example of a rough cross-section and simplified cross-section for ESL2. The shaded area is the roughness-area, used in the statistical analysis.

Table I. Summary table showing significant reach averaged values for each reach

Reach[a]	Channel type	Average Q (m^3/s)	Gradient (m/m)	D_{84} (m)	σ^b	CV[c] of R/D_{84}	Average roughness-area (m^2)	CV roughness	Wood volume/area (m^3/m^2)	Pool volume/area (m^3/m^2)	CVPoolV
ESL1	step-pool	0·34	0·09	0·16	0·51	0·36	0·51	0·80	0·0051	0·27	0·06
ESL2	step-pool	0·37	0·09	0·07	0·85	0·19	0·37	0·62	0·0169	0·22	0·35
ESL3	cascade	0·40	0·13	0·13	0·34	0·12	0·77	0·56	0·0014	0·05	0·33
ESL4	step-pool	0·38	0·12	0·17	0·39	0·20	0·33	0·90	0·0017	0·22	0·28
ESL5	cascade	0·39	0·14	0·14	0·45	0·21	0·52	0·86	0·0093	0·09	0·31
ESL6	plane-bed	0·88	0·02	0·09	0·65	0·24	0·11	0·56	0·0028	–	–
ESL7	cascade	0·41	0·09	0·17	0·33	0·23	0·29	0·65	0·0084	–	–
ESL8	step-pool	0·36	0·09	0·17	0·39	0·16	0·37	0·88	0·0118	0·13	0·07
ESL9	step-pool	0·33	0·11	0·15	0·40	0·16	0·37	0·72	0·0067	0·24	0·10
FC1	step-pool	0·12	0·06	0·08	0·43	0·39	0·07	0·72	0·0007	0·09	0·28
FC2	step-pool	0·10	0·07	0·08	0·43	0·43	0·08	0·67	0·0029	0·12	0·59
FC3	step-pool	0·09	0·09	0·05	0·70	0·41	0·15	0·86	0·0090	0·08	0·89
FC4	step-pool	0·13	0·13	0·10	0·30	0·37	0·21	0·67	0·0058	0·12	0·37
FC5	cascade	0·04	0·16	0·09	0·48	0·38	0·06	1·11	0·0074	0·03	0·14
FC6	cascade	0·04	0·18	0·09	0·26	0·35	0·06	0·92	0·0006	0·04	0·29

[a] ESL = East St Louis Creek and FC = Fool Creek, ESL1 and FC1 are both the furthest downstream reach and ESL9 and FC6 are the furthest upstream.
[b] $\sigma = \log(D_{84}/D_{50})$ = bed material size distribution.
[c] CV = coefficient of variation.

other parameters, e.g. wood, influence the combined variations in the three hydraulic geometry exponents. Compositional data are best represented by ternary diagrams, which were simultaneously introduced by Park (1977) and by Rhodes (1977). The exponents, *b*, *f*, and *m* are all dependent on each other, so Ridenour and Giardino (1991) argue that they should be analyzed simultaneously. Therefore, we use principal component analysis (PCA) to describe the combined rates of change of width, depth and velocity for each segment of channel, and use the axis scores in a multiple regression analysis to better understand what influences the variability in these exponents.

Another method of understanding the simultaneous variability in the hydraulic exponents is by analyzing the ternary diagrams. Rhodes (1977) proposed five subdivisions of the diagram which represented width-depth ratio ($b = f$), competence ($m = f$), Froude number ($m = f/2$), velocity-cross-sectional area ratio ($m = b + f$), and slope-roughness ratio ($m = 2/3\ f$). The last two are related to the Darcy–Weisbach friction factor and Manning equation (n), respectively. The streams that plot together on the ternary diagram are expected to have similar responses to an increase in discharge. Park (1977), however, found a large range of AHG values over varying climatic regions. Subsequently, Park (1977) concluded that local controls may have a larger influence on AHG values than climatic controls.

The objectives of this study are to (1) report at-a-station values for cascade, step-pool and plane-bed reaches and determine whether there are significantly different values for cascade versus step-pool reaches (plane-bed not included in statistical comparison since sample size = 1); and (2) explore what influences the variability in the rate of change of width, depth and velocity with discharge. These objectives can be separated into two hypotheses: (i) there is a significant difference between hydraulic geometry exponents for cascade versus step-pool reaches; and (ii) the variability in the hydraulic geometry exponents are significantly related to the following potential control variables: bed gradient, channel roughness, wood load, and pool volume. The AHG for the single plane-bed reach is used for comparison with data collected from plane-bed reaches in British Columbia (Reid, 2005; Reid and Hickin, 2008).

Study Site

East St Louis Creek (ESL) and Fool Creek (FC) are located in Fraser Experimental Forest in the Colorado Rockies 112 km west-northwest of Denver (Figure 2). Elevations range between 3925 m at the top of FC to 2895 m at the bottom of ESL. Vegetation varies from Engelmann spruce and subalpine fir at higher elevations to lodgepole pine at lower elevations. Alpine tundra can also be found at the higher elevations in both basins. Runoff is dominated by snowmelt with small contributions by summer convective storms (Trayler and Wohl, 2000). Average annual precipitation over the entire forest is 787 mm (USDA Forest Service, 2009). Historically, peak discharges occur in mid-June, with 80% of the total flows occurring between April and October (Wilcox and Wohl, 2006).

Each creek is in a confined valley surrounded by Pleistocene and Holocene lateral moraines and underlain by Pre-Cambrian biotite-gneiss and Silver Plume granite (Taylor, 1975). Both basins have shallow soils with low silt/clay content that are mainly derived from gneiss and schist (USDA Forest Service, 2009).

ESL drains approximately 8·73 km^2 and has been gaged since 1943. Lower Fool Creek (LFC), which includes the Upper Fool Creek (UFC) basin, drains 2·89 km^2 and has been gaged since 1941. UFC is a 0·69 km^2 basin with a gage installed around 1986. All of the basins are dominated by cascade and step-pool morphologies above the gages, with limited plane-bed reaches. Only one plane-bed reach was found on ESL for the purposes of this study.

Table I shows the average values for all of the potential control variables for each reach. The step-pool reaches have steps formed from wood jams and from boulders. The steps formed from large wood jams usually have at least one large keystone boulder associated with them. The largest steps are associated with large wood jams and are found on ESL2, the upstream section of ESL5 and FC3. The sections above these steps have reduced gradients and deposition of finer sediment. ESL5 has the largest step height at the top of the reach and directly above it is the plane-bed reach (ESL6). Nappe flow was observed over all steps at all flows, although some of the smaller steps in each reach were submerged at the highest flows (Chanson, 1994; Church and Zimmerman, 2007; David *et al.*, 2010). FC1 had small cobble steps in the downstream portion of the reach that were sub-

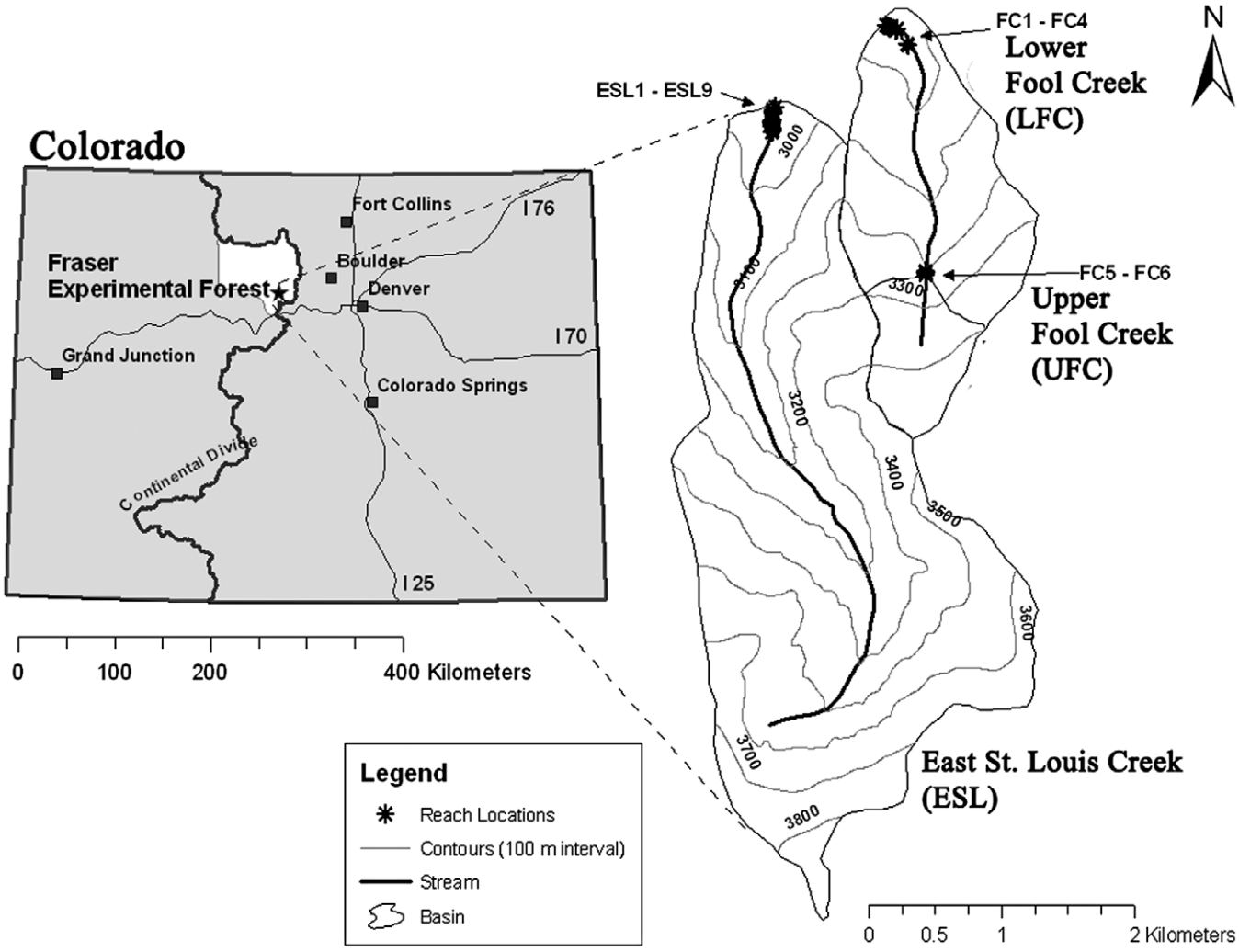

Figure 2. Location map of East St Louis Creek (ESL) and Fool Creek (FC) in Fraser Experimental Forest, Colorado. Fool Creek is divided into two basins: Lower Fool Creek (LFC) and Upper Fool Creek (UFC).

merged at the highest flows. The average percent difference between the water-surface slope (S_w) and the bed slope (S_0) is 4·2%, with the highest percent difference in the plane-bed reach with an average difference of 22·9% over the four flow periods. The average percent difference in the step-pool and cascade reaches is 2·8 and 2·6%, respectively.

ESL5 and ESL7 had changes in the wood load between 2007 and 2008. ESL5 had the largest change with an additional log in the reach in 2008. ESL7 has the largest amount of logs bridging the reach and some of these broke before the 2008 survey. FC3 had overbank flow during the 2008 high flow, which notably widened the reach and allowed a small island to develop in the middle of the channel. The flow went back to the main channel once the snowmelt period was complete. ESL1 and ESL4 also had some slight overbank flow during the peak runoff period but the majority of the water remained within the main channel.

Methods

Field methods

The water-surface elevation and velocity were measured on 15 channel reaches on ESL and FC. Reach lengths were determined based on consistent morphology throughout the reach. Rebar was placed in the thalweg at the upstream and downstream end of each reach. The hydraulic variables were measured over two summers (2007 and 2008) and four flows (July 2007, August 2007, June 2008, July 2008). A laser theodolite was used to collect both the bed and water-surface data every 15 cm along the thalweg and banks of each reach. The reach-average mean velocity was measured using Rhodamine WT dye tracer and fluorometers attached to upstream and downstream rebar. The fluorometers were placed at 0·6*h* from the water surface for each measurement. Two velocity replicates were completed before surveying the reach and two after. All four of these were averaged for the mean velocity. The differences between the centroids of the mass of dye were used, rather than the difference between peaks, for determining the time difference between the two probes (Lee and Ferguson, 2002; Curran and Wohl, 2003; David, 2010). The standard deviation of velocity measurements ranged from 0·001 m/s to 0·34 m/s, with the greatest variation between measurements occurring at high flows. The instantaneous gage data over the time of the survey show a larger fluctuation in discharge during the snowmelt period (June 2008) than later in the season (July 2007, July 2008, August 2007).

A Wolman (1954) pebble count of 300 pebbles was conducted during the August low flow period to determine particle size and sorting. The intermediate axis of each clast was measured with a ruler along equally spaced transects. Many of the largest boulders (0·5–1 m) were partly embedded, therefore the length of the intermediate axis was approximated. A

pebble count was repeated in August 2008 in one step-pool, cascade and plane-bed reach and average errors of 13, 8 and 4%, respectively, were determined for each channel type.

The channel geometry measurements were made using a tripod-mounted Light Detection and Ranging (LiDAR) unit during the low flow period in August 2007. Each individual scan was merged within a tolerance of 1 cm at the control points. The pointcloud density varied substantially in each reach. The LiDAR scans were coupled with a feature-based survey with variable gridding that depended upon the underwater features, which was completed with a laser theodolite. The water-surface data were imported into the scans and cross-sections were created using Cyclone 5.8.1 (Leica Geosystems, 2008). The cross-sections were equally spaced in each reach and dimensions imported into a spreadsheet in Microsoft Excel. The average water-surface elevation was determined for each cross-section and used to calculate the channel geometry data, i.e. width (w), depth (h), hydraulic radius (R), and cross-sectional area (A). Values for each of these variables are reach averages based on multiple cross-sections spaced at 1 m intervals. The water-surface slope (S_w) and bed slope (S_0) were calculated for each reach using a linear regression of the thalweg on the laser theodolite surveys. The water-surface slope (S_w) was used to calculate the Darcy–Weisbach friction factor. Although it is understood that slope adjusts along with all other hydraulic variables, over the short time scale considered the bed slope (S_0) is considered static and treated as a potential control variable.

The average projected wetted roughness-area (A_R) was calculated for each reach (Figure 1), using a similar method as Bathurst (1985). A simplified cross-section was created for each cross-section by connecting successive low points with straight lines. A macro in Visual Basic Editor was used to connect these points by finding the steepest slopes between two survey points and drawing a line between these points (David, 2010). The flow cross-sectional area (A) was subtracted from the simplified cross-sectional area (A_s) as a means of defining the roughness cross-section area (Figure 1). The roughness cross-section area is used as another means of defining the area of boulders and logs that project into the flow, increasing flow resistance. Because multiple cross-sections were used for each at-a-station value, the coefficients of variation of the roughness-area as well as the average roughness-area were compared to the hydraulic exponents.

The total wood volume was calculated using the LiDAR scans. The length and diameter of wood was measured for any piece below the highest flow. The volume for each piece was calculated and then summed for a total volume for that reach. The total wood volume was then divided by the plan area of the reach to get the volume per squared meter of the reach. Therefore, the different lengths of the reaches are accounted for in this value. The pool volume was estimated using the product of the length, maximum depth and average width. This value was calculated for each flow period. The volume per squared meter and the coefficient of variation of the pool volume (CVPoolV) were used in the statistical analysis described later. The total volume is dependent on reach length; therefore it was not included in the regressions. The coefficient of variation (CV) is equal to the standard deviation over the four flow periods divided by the mean pool volume. The average values of these variables are shown in Table I.

Statistical methods

A PCA was used in Multivariate Statistical Package (MVSP) using a sample size of 15 (Kovach Computing System, 2002). PCA is an ordination technique that rearranges the data into a smaller set of composite variables (McCune and Grace, 2002). This method uses an orthogonal linear transformation of the data, in which the greatest variation in the data lies on the first axis, or principal component. Each principal component minimizes the total residual sum of squares of the eigenvector (taken from the covariance matrix), after passing through the means of the eigenvalues (McCune and Grace, 2002). Since the three AHG exponents are interrelated, a PCA is used to reduce the redundancy for all 15 reaches into principal components which accounts for most of the variance in the AHG exponents.

A best subsets regression was performed using the program R (R Core Development Team, 2007; Kutner *et al.*, 2005) to determine which independent variables best explained the variability in hydraulic exponents. The roughness-area, bed gradient, CVPoolV, pool volume per squared meter of reach, wood volume per squared meter of reach, D_{84}, bed-material size-distribution (σ) and standard deviation of bed elevation were all regressed against the PCA Axis 1 scores in a best subsets regression. A best subsets was also used in a regression for the individual AHG exponents and each of the above explanatory variables, to explore if the same explanatory variables are significantly related to individual exponents. A Tukey HSD (honestly significant difference) method was used to test for significant differences between means in an ANOVA (analysis of variance) comparing the exponents for step-pool versus cascade reaches. The Tukey HSD method adjusts for differences in sample sizes, so appropriate comparisons can be made between means (R Core Development Team, 2007).

Outliers in the regressions were examined using a number of diagnostic techniques. First, studentized residuals were examined for each regression, followed by the leverage (h_{ii}), DFFITS, DFBETAS and Cooks Distance (Kutner *et al.*, 2005). Each diagnostic was considered carefully. In many cases, ESL3 was found to cause regression assumptions to be violated and therefore was removed from consideration in the regressions. Outliers were only removed after it was determined that the sample was highly influential, with high leverage, on the regression.

Ternary diagrams are used as a means of comparing the exponents (m, f, b) for each reach and each channel type. The AHG values found in this study are compared to Reid's (2005) study on streams in British Columbia. All three AHG exponents are interrelated; therefore, the ternary diagram has been found to be a useful format for investigating simultaneous variations in the exponents (Park, 1977; Rhodes, 1977). The sum of the exponents did not equal unity for a majority of the reaches; therefore, the values of the exponents for an individual reach were proportionally adjusted until the exponents summed to unity.

Results

AHG is not significantly different among step-pool, cascade and plane-bed reaches at ESL and FC (Figures 3 and 4 and Table II). These results do not support the hypothesis that there is a significant difference in hydraulic exponents for cascade and step-pool reaches. For all reaches except two, the at-a-station values show that $m > f > b$ (Table II and Figure 4), indicating that the rate of change of velocity with discharge is greater than the rate of change of width or depth. The mean values of 0·49 for m, 0·35 for f and 0·16 for b are within the mean and range found by Comiti *et al.* (2007) and other researchers (Lee and Ferguson, 2002; Bathurst, 1993) who have studied step-pool and cascade systems. The at-a-station

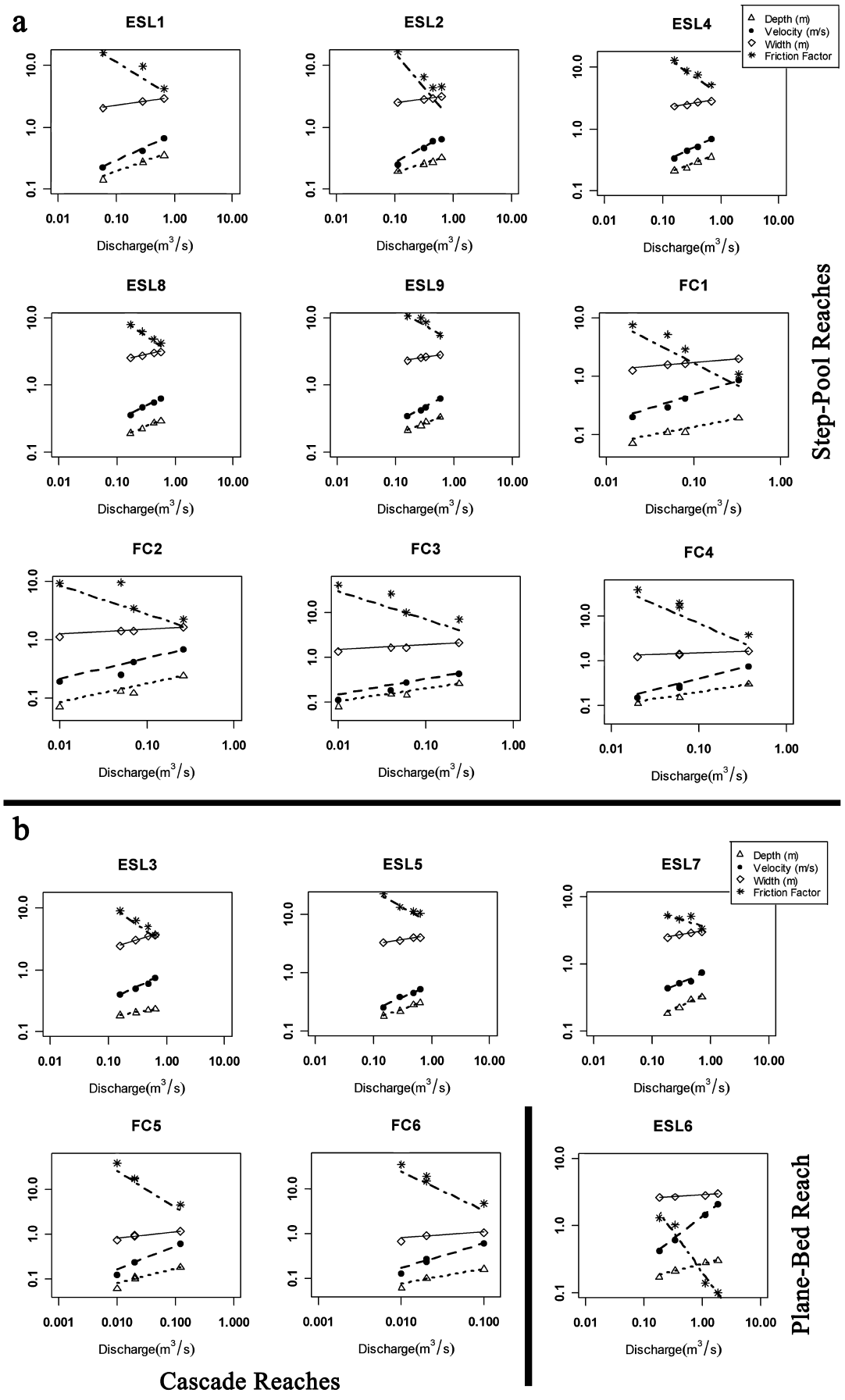

Figure 3. (a) AHG of each step-pool reach and (b) AHG of each cascade reach and the plane-bed reach (ESL6). The power relationships between discharge and velocity (*m*), depth (*f*), width (*b*) and the Darcy–Weisbach friction factor (*x*) are shown on each graph.

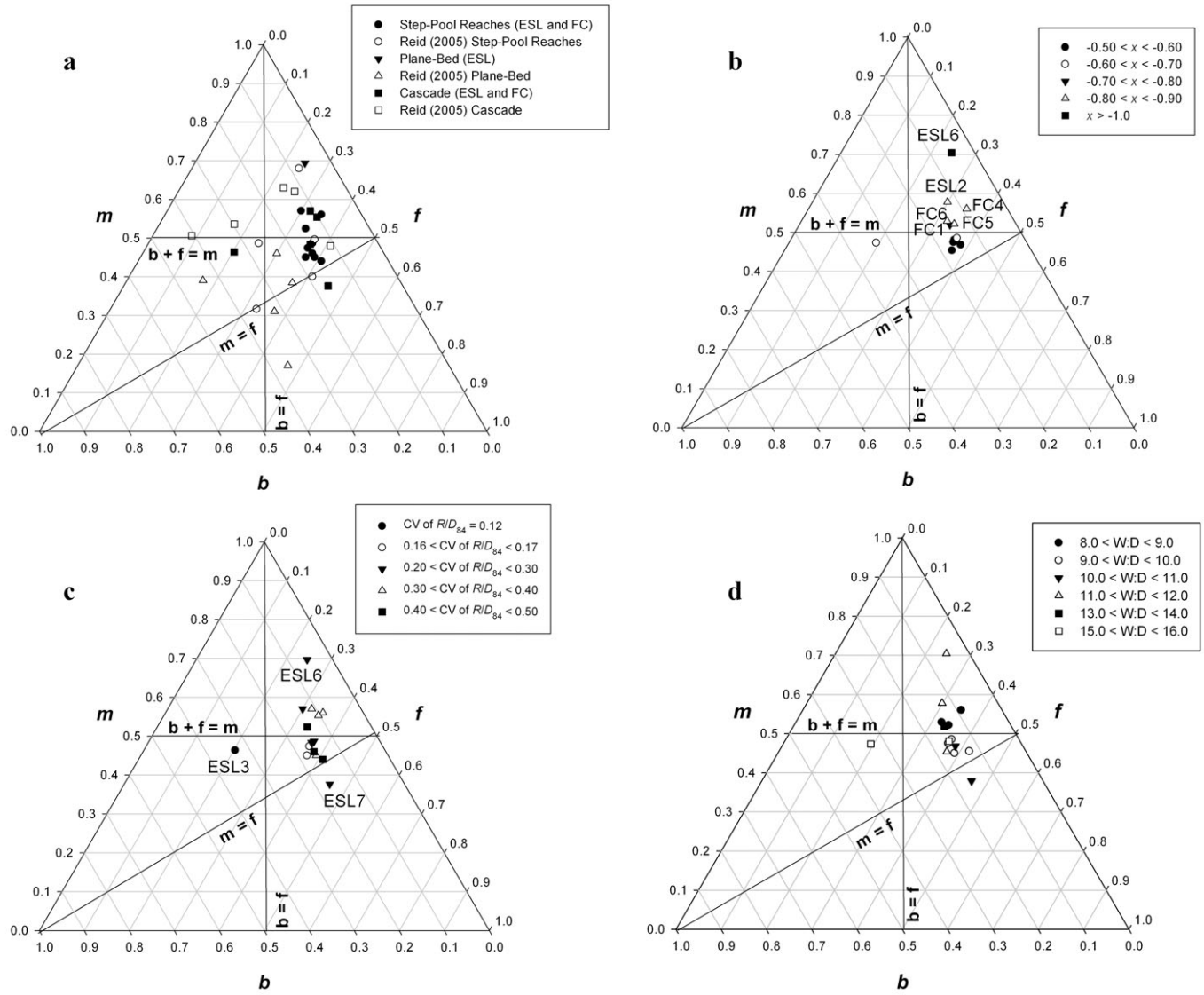

Figure 4. *b*–*f*–*m* ternary diagrams: (a) step-pool and cascade reaches in comparison to Reid's (2005) study; (b) reaches with particular rates of change of the Darcy–Weisbach friction factor (x); (c) reaches with a particular coefficient of variation of R/D_{84}; (d) reaches with a particular width/depth ratio.

values are significantly related to average roughness-area and the bed gradient (Table III), supporting the second hypothesis that channel roughness and bed gradient explain the variability in at-a-station values, although these results are tempered by the small sample size (n = 15) used in this study. A more detailed presentation of the results follows in three sections: (i) a summary of the at-a-station values found in these reaches; (ii) channel type versus AHG; (iii) controls on AHG.

Summary of AHG

The mean values of each of the exponents are 0·49 for m, 0·35 for f and 0·16 for b (Table II). All exponents were significant at the $\alpha = 0{\cdot}05$ level except for the b value in FC6. All regressions were significant at the $\alpha = 0{\cdot}05$ level, but some of the intercepts were not significant, probably because of the low degrees of freedom in each regression related to the sample size of four used in each AHG regression. Because of the lack of significance of many of the coefficients, these were not analyzed separately. Despite the low degrees of freedom, the coefficient of determination is high for almost all the regressions, indicating a good fit of the data (Figure 3). In most cases $m + f + b$ does not equal one, but this is most likely an artifact of using average reach cross-sections rather than individual cross-sections for the analysis.

The mean, standard deviation and range of values for m are similar to the values found for step-pool and cascade reaches in the Rio Cordon (Comiti *et al.*, 2007) and other step-pool and cascade streams (Lee and Ferguson, 2002; Bathurst, 1993). The range of values found in Colorado was also similar to the range found by Reid (2005) for lower gradient step-pool, cascade and plane-bed reaches in British Columbia (Figure 4a), although there was a larger amount of scatter in Reid's data and the means differed (m = 0·51, f = 0·29, b = 0·20).

Differences in the rate of change of depth and width with discharge may be related to differences in channel shape and roughness. For ESL2, ESL6, FC1, FC4, FC5, and FC6, m is greater than $b + f$, indicating that the velocity is increasing faster than the flow area in these reaches. The width exponent signifies that there is not a large variation in width between low and high flows for a majority of the reaches despite changes in some reaches because of bank undercutting.

The at-a-station values indicate that for a majority of the reaches $m > f > b$. Therefore, the velocity increases faster with

Table II. Summary table showing the power relationships between Q versus w ($w = aQ^b$) (width), Q versus d ($d = cQ^f$) (depth), Q versus v ($v = kQ^m$) (velocity), and Q versus ff (ff = oQ^x) (friction factor)

Reach	Channel Type	Width			Depth			Velocity			Friction factor			Width/depth ratio	ff	R/D_{84}	Number of cross-sections
		a	b	R^2	c	f	R^2	k	m	R^2	o	x	R^2				
ESL1	step-pool	3·13*	0·16*	0·99	0·42*	0·39*	0·99	0·76	0·45*	0·99	3·98	–0·53	0·90	8·43 14·03	4·23 16·32	1·62 0·75	27
ESL2	step-pool	3·33*	0·12*	0·97	0·35*	0·29*	0·98	0·26	0·56*	0·98	2·64*	–0·82*	0·95	9·95 13·71	4·35 16·84	3·51 2·18	18
ESL4	step-pool	3·04*	0·15*	0·99	0·40*	0·37*	0·97	0·15*	0·49*	0·98	4·09*	–0·62*	0·98	8·22 11·07	5·17 13·15	1·52 0·99	15
ESL8	step-pool	3·48*	0·17*	0·99	0·36*	0·36*	0·99	0·80*	0·44*	0·99	3·09*	–0·54*	0·99	10·84 13·44	4·22 8·05	1·35 0·93	20
ESL9	step-pool	3·09*	0·16*	0·98	0·41*	0·36*	0·99	0·79*	0·47*	0·99	4·54*	–0·52*	0·88	8·45 10·93	5·60 10·78	1·64 1·11	16
FC1	step-pool	2·36*	0·15*	0·97	0·28*	0·34*	0·97	1·53	0·53*	0·99	0·50*	–0·72*	0·98	10·21 18·46	1·07 7·58	1·95 1·15	22
FC2	step-pool	1·91*	0·11*	0·98	0·37*	0·37*	0·96	1·08	0·40*	0·90	1·35	–0·46	0·71	6·91 16·37	2·23 9·59	2·16 0·74	14
FC3	step-pool	2·53*	0·14*	0·97	0·43*	0·36*	0·97	0·82	0·44*	0·97	2·91	–0·58*	0·86	8·11 16·14	7·24 42·13	3·83 1·44	15
FC4	step-pool	1·83*	0·09*	0·96	0·41*	0·35*	0·99	1·28*	0·56*	0·99	1·76*	–0·81*	0·99	5·50 11·18	3·82 39·89	2·14 0·95	17
ESL3	cascade	4·30*	0·31*	0·98	0·25*	0·18*	0·99	0·86*	0·44*	0·99	3·00*	–0·62*	0·98	15·54 13·34	3·75 9·15	1·39 1·07	13
ESL5	cascade	4·37*	0·16*	0·99	0·36*	0·37*	0·99	0·66*	0·49*	0·98	7·80*	–0·53*	0·94	13·40 18·26	10·66 22·85	1·66 1·03	16
ESL7	cascade	3·24*	0·15*	0·96	0·38*	0·44*	0·98	0·78	0·36*	0·92	3·45*	–0·27	0·58	9·32 13·56	3·34 5·26	1·45 0·86	17
FC5	cascade	1·66*	0·16*	0·90	0·45	0·40*	0·90	2·32	0·61*	0·96	0·76	–0·83*	0·99	6·23 12·11	4·64 39·22	1·43 0·59	15
FC6	cascade	1·68*	0·18	0·77	0·42	0·39*	0·91	2·82	0·64*	0·96	0·63	–0·86*	0·98	6·59 10·97	4·73 36·16	1·22 0·52	19
ESL6	plane-bed	2·86*	0·05*	0·96	0·27*	0·24*	0·99	1·33*	0·69*	0·99	0·20*	–1·22*	0·96	9·88 15·99	0·10 1·31	3·04 1·75	9

Note: The coefficient of determination (R^2) is shown for each power relationship. The minimum and maximum values of width/depth ratio, ff, and R/D_{84} that were found over the four flow periods of measurement. The number of cross-sections used to determine average values for width and depth are also shown. The number of cross-sections varied based on reach lengths. The values for width/depth ratio, ff and R/D_{84} are the values at high flow (top) and low flow (bottom) for each reach.
* Significant at the level of $\alpha = 0{\cdot}05$.

Table III. Results of best subsets regressions for PCA Axis 1 scores, the velocity exponent (m) and friction exponent (x) versus significant explanatory variables

	Independent variables[b]						
Dependent variables[a]	Intercept	Roughness-area	Gradient	CVPoolV[c]	D_{84}	p-Value	Adjusted R^2
PCA Axis 1 scores[d]	0·14	–0·05	0·36	n.s.	n.s.	0·0007	0·68
Velocity exponent (m)[e]	0·42	n.s.	1·60	n.s.	–0·82	0·005	0·59
Friction exponent (x)[f]	–0·65	0·43	n.s.	–0·67	n.s.	0·04	0·59

Note: There were no significant regressions found using the width and depth exponents; n.s. = not significant.
[a] No significant regressions were found using the width and depth exponents (b, f) as dependent variables.
[b] Wood volume per squared meter, $\log(D_{84}/D_{50})$ and width/depth ration were all not significant in any regressions.
[c] CVPoolV = Coefficient of variation of pool volume.
[d] ESL3 and ESL6 both removed from regression as outliers (n = 13).
[e] FC1 and FC3 may have high leverage in this regression and could be driving the results, but were not removed from the regression (n = 15).
[f] ESL1, ESL7, FC2 excluded because exponents not significant in at-a-station regressions. ESL6 and FC3 excluded because both are outliers and have high leverage on regression (n = 10).

discharge than does depth, and depth increases faster than width for all reaches except ESL3 ($b > m > f$) and ESL7 ($f > m > b$). ESL3 is the only reach that has a width/depth ratio that increases with discharge (Table II). The shape of the channel is very different from the other reaches because of a bar the same length of the reach which has large boulders and even some herbaceous vegetation that splits the flow. The left bank of this reach is also noticeably steep and unstable, with most of the wood being input from this bank. An increasing width/depth ratio with discharge means that the flow is primarily accommodated by an increase in width rather than an increase in depth in this reach.

All reaches except ESL7 have $m > f$, which can be interpreted as increasing stream competence with increasing discharge (Rhodes, 1977; Reid, 2005), although this subdivision is related to low gradient streams and does not account for bed armoring in these higher gradient channels. ESL7 is the only reach that has depth increasing faster with discharge than velocity. The increase in depth may be related to increased roughness from wood as discharge increases in this reach. Much of the roughness associated with wood in this reach is from overhanging branches that become submerged at higher flows. The channel shape in this reach is also different from the other reaches, with nearly vertical banks on both sides that enhance stage changes with increasing discharge.

The rate of change of the friction factor with discharge (x) is higher than all other exponent values ($x > m > f > b$). The values of the friction factor exponents were not significant for ESL1, ESL7 and FC2, therefore the rate of change of friction factor with discharge may not be the same power relationship for these three reaches as for the other 12 reaches (Figure 3). The rate of change of friction factor is highest for the plane-bed reach and lowest for ESL5 and ESL9. Figure 3 and the ternary diagrams (Figure 4b) indicate a relationship between the rate of change of friction factor and the combined hydraulic geometry exponents. In particular, as the rate of change of velocity and depth increases, the friction factor decreases more rapidly.

Figures 4(c) and 4(d), respectively, show the CV of R/D_{84} and the width/depth ratio for the same reaches. The CV of R/D_{84} is used as a measure of the variability in the protrusion of roughness elements over the four flow periods. Generally, reaches with lower variability (CV of $R/D_{84} < 0{\cdot}17$) plot below the $b + f = m$ line, but reaches with a higher coefficient of variation (CV of $R/D_{84} > 0{\cdot}20$) plot over a larger range. In Figure 4(d) reaches with similar width/depth ratio generally plot together, but there was no particular trend in terms of location of those points on the ternary diagram.

Channel type and AHG

The ternary diagrams (Figure 4), PCA (Figure 5) and boxplots (Figure 6) indicate that there is no significant difference among hydraulic exponents between step-pool and cascade channel types. The lack of relationship can also be a result of the small sample size, with only five cascade and nine step-pool reaches. The width exponent (b) is significantly different between step-pool and cascade reaches. In all probability the width exponents are significantly different because of the much larger rate of change of width with discharge for ESL3. Therefore, these results do not support the first hypothesis that the hydraulic geometry exponents are significantly different between step-pool and cascade reaches. Another analysis with a larger dataset should be completed to further test this conclusion.

Potential controls on AHG

A PCA was conducted using the three AHG exponents. The axis scores for each reach represent the combined width, depth and velocity exponents for that reach. The scores on Axis 1 (Figure 5) explain the majority of the variability in the dataset (~97%) and are mainly related to the velocity and depth exponent. Very little of the variability is explained by the width exponent.

The regression of PCA Axis 1 scores shows that roughness-area and gradient are significantly related to the rates of change of velocity, depth and width with discharge (Table III). ESL3 and ESL6 were consistently outliers and removed from the regression. The diagnostic tools used to identify outliers are described earlier. Despite the small sample size in this regression (n = 12), the power, p-value and R^2 indicate that this is a significant result.

The individual exponents were examined in separate regressions to determine if individual exponents were similarly related to the explanatory variables (Table III). Roughness-area is also significantly related to the friction exponent. Wood volume per squared meter of reach is not significant in any regression. The D_{84} and gradient are both significantly related to the velocity exponent. These results support the hypothesis that the exponent values are significantly related to control variables that represent both resisting forces (roughness-area) and driving forces (gradient).

Table III also shows that the friction exponent is significantly related to roughness-area and the variability in pool volume

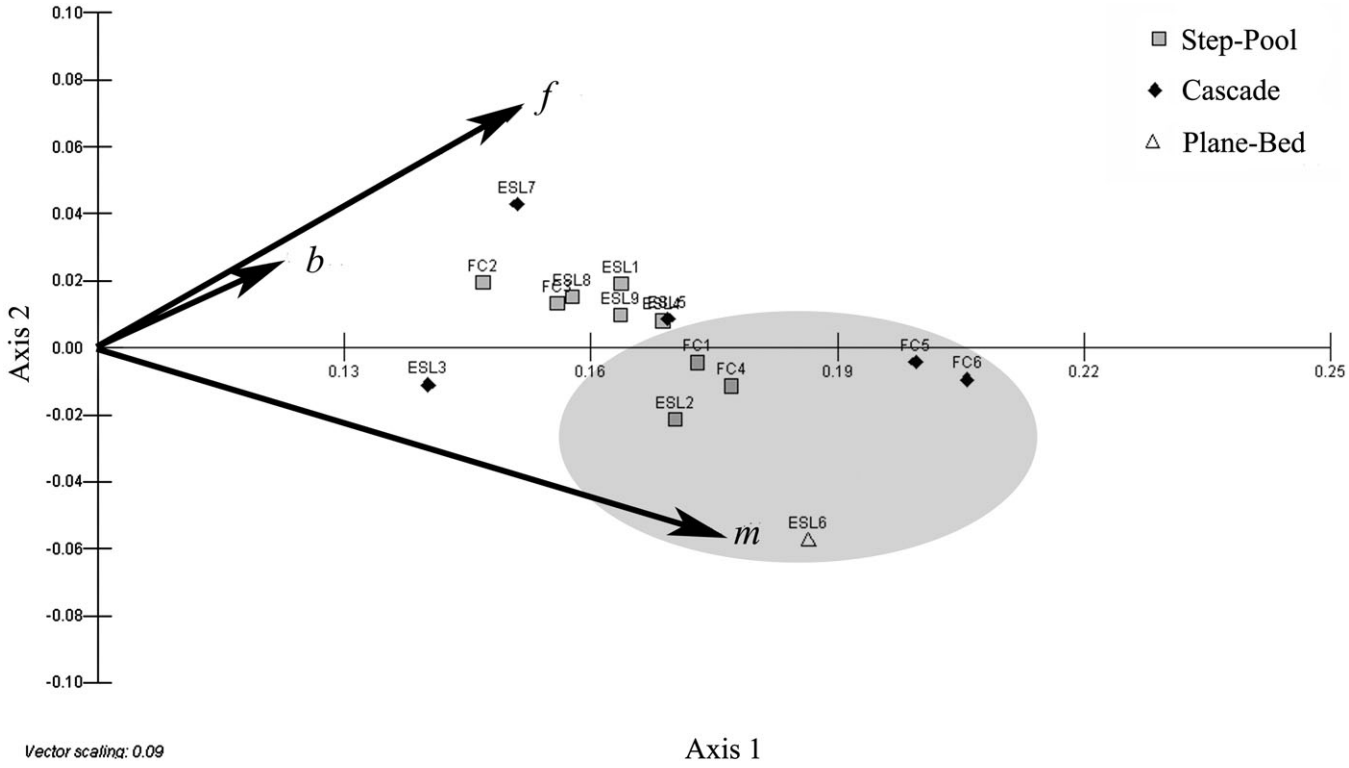

Figure 5. PCA of all 15 reaches using *m*, *f*, and *b*. The shaded area shows the reaches that have the most similar characteristics both in the ternary diagram and are interpreted to be dominated by grain resistance.

(CVPoolV). These regressions indicate that roughness-area may be a better measure of bed roughness than grain size. PCA Axis 1 scores were also significantly related to the friction exponent (Figure 7). The rate of change of the friction exponent is larger for higher PCA Axis 1 scores, which is related to higher *m* values. Although there may be differences in this relationship based on the differences between basins or channel types (Figure 7), more cascade reaches would need to be included in the analysis to determine whether there is in fact a significantly different relationship. The steeper slope for both the cascade reaches and the Fool Creek reaches in the scatter plot is probably related to the steeper gradient of both FC5 and FC6.

Scatter plots (Figure 8) of PCA Axis 1 versus roughness-area, wood volume per squared meter, coefficient of variation of R/D_{84} and CVPoolV show that the relationships between each variable and the PCA axis scores may not be best represented by a log-linear regression. As the roughness-area increases, the variability in PCA Axis 1 scores decreases (Figure 8a). Therefore, there is more variability in the rates of change at a lower average roughness-area. The relationship between the coefficient of variation of R/D_{84} and PCA Axis 1 is positive for the ESL reaches, except for ESL1, and negative for the FC reaches (Figure 8b). The coefficient of variation is much higher for the FC reaches than for the ESL reaches. This means that there is a larger standard deviation and lower mean value of relative submergence over the four flow periods in FC than in ESL. Further work needs to be done to determine if these trends persist with a larger sample size.

The CVPoolV represents the variability in pool size as flow changes for each reach. There is no significant relationship between this variable and PCA Axis 1 score (Figure 8c), although a relationship may exist between CVPoolV and the FC reaches. Both Figures 8(b) and 8(c) underscore the differences between basins and the variability in these relationships even in adjacent basins.

The variability in PCA Axis 1 scores is reduced at higher values of wood volume per squared meter (Figure 8d); for both low values of roughness-area and wood volume per squared meter, there is much higher variability in rates of change of velocity and depth with discharge. At higher values the total friction increases and the velocity and depth do not vary as much between low and high flows. In reaches with higher values of wood volume per squared meter, the roughness would increase with flow as more wood becomes submerged. Therefore, the contribution of roughness from wood may either increase, or remain the same between low and high flows.

Figure 9 shows each of these variables in a bar plot for a better understanding of the magnitude of differences among reaches. The wood load and pool volume per squared meter vary the most among reaches, with FC1 through FC4 having similar values of pool volume per squared meter. The average gradient gradually increases moving upstream from FC1 to FC6. The ESL reaches do not follow such a consistent trend and are much more similar in gradients except for the one plane-bed reach (ESL6). The D_{84} is similar for most of the FC reaches except for FC3. The same is true for the ESL reaches, except for ESL2 and ESL6. These bar plots and a correlation matrix (Table IV) also help in understanding the interactions between these variables. The two reaches in each basin with the highest wood load (ESL2, FC3) also have the lowest values of D_{84}. Table IV displays a slight correlation between wood load and pool volume per squared meter. The majority of the wood found in the step-pool reaches is located in the steps. Since each pool is associated with a step, it is expected that there would be some interrelationship between pools, steps and wood. There is also a slight correlation between pool volume per squared meter and D_{84}, but no correlation exists between D_{84} and wood volume per channel area.

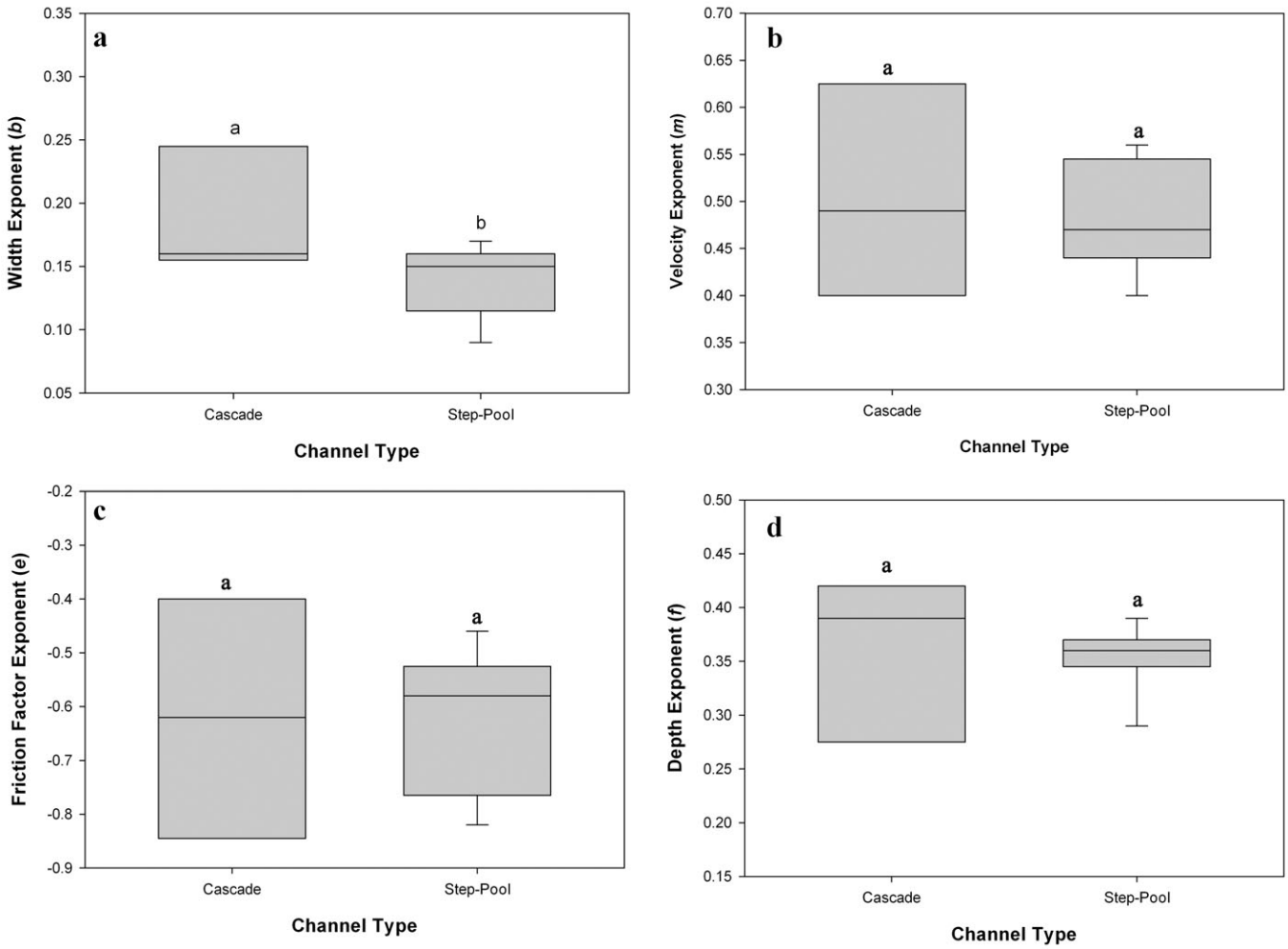

Figure 6. Boxplots showing (a) the range of values of the width exponents (*b*) for step-pool and cascade reaches; (b) the range of values for the velocity exponents (*m*) for step-pool and cascade reaches; (c) the range of values for the depth exponents (*f*) for step-pool and cascade reaches; (d) the range of values for the friction factor exponents (*x*) for step-pool and cascade reaches. The letters a and b above the boxes show the results of the ANOVA and Tukey HSD test. If the same letters are above the boxes then the average value of the exponents for those two channel types are not significantly different from each other, if different letters are above the boxes then they are significantly different from each other.

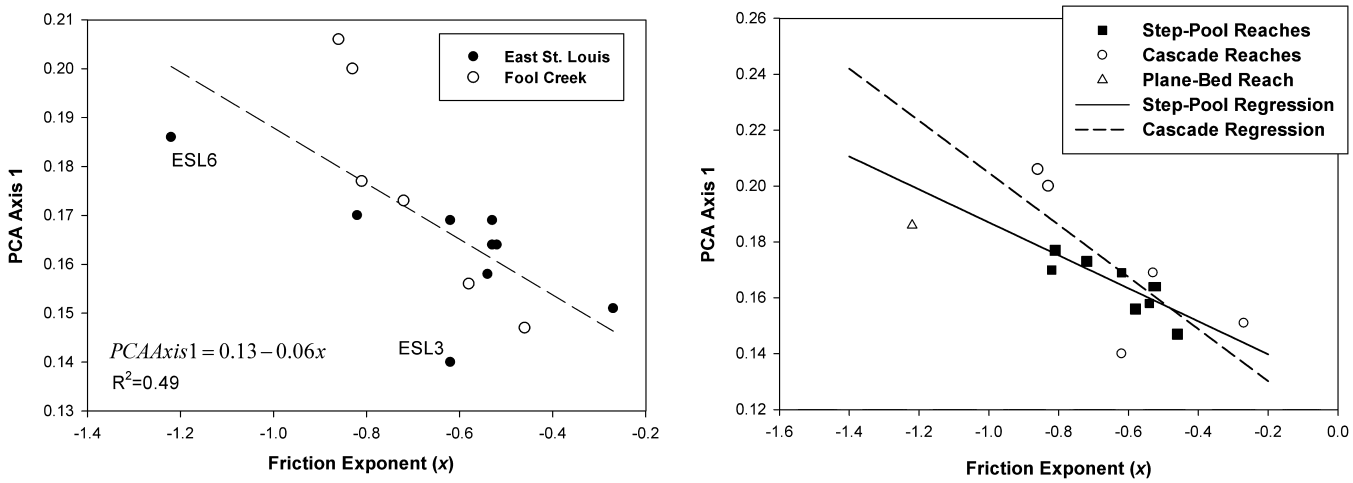

Figure 7. The PCA Axis 1 scores against the Darcy–Weisbach friction factor exponent (*x*) divided by drainage basins (left) and channel type (right).

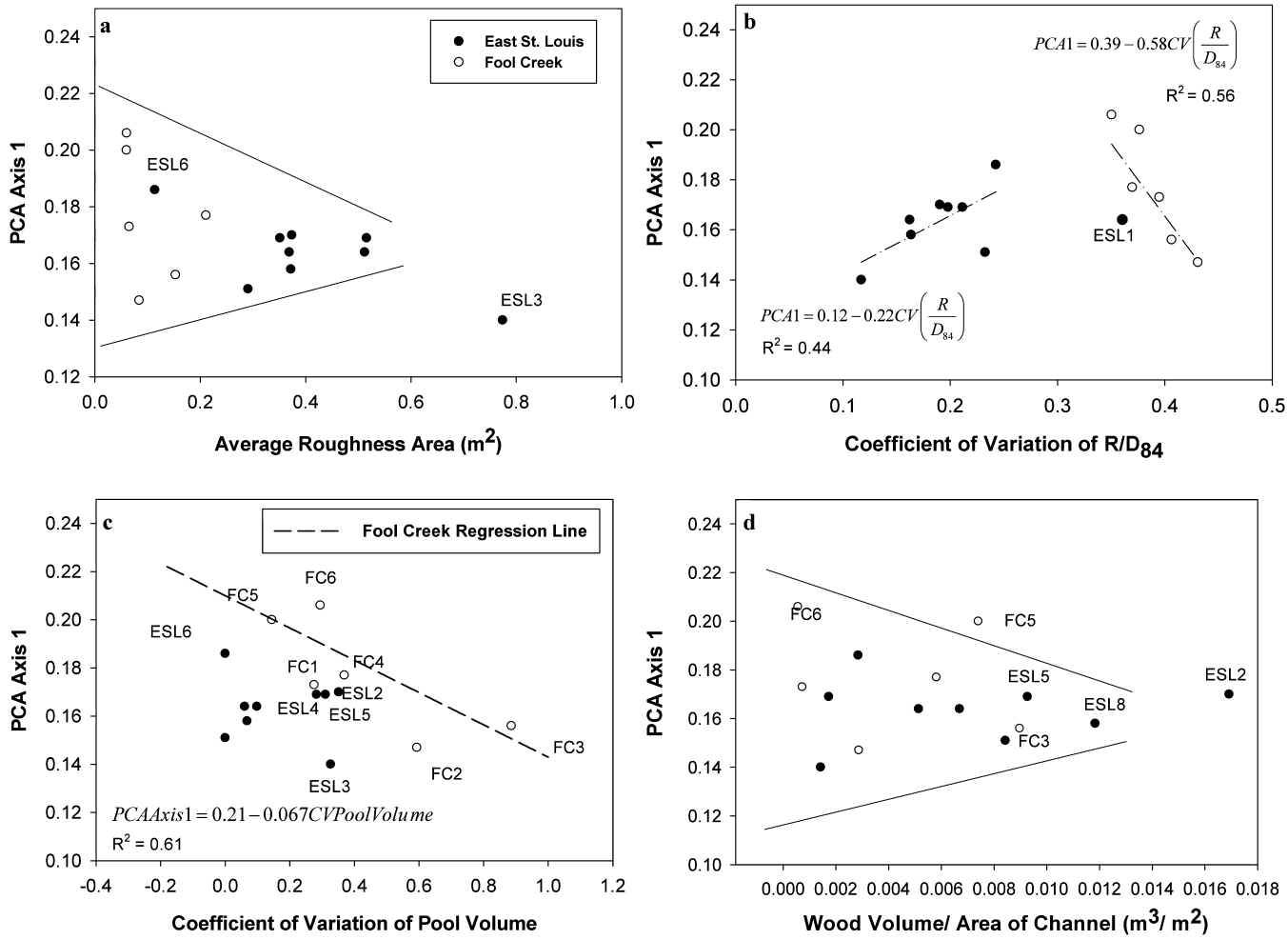

Figure 8. PCA Axis 1 scores versus (a) average roughness-area, (b) coefficient of variation of R/D_{84}, (c) coefficient of variation of pool volume and (d) wood volume per channel area for the two drainage basins (ESL and FC).

Discussion

AHG versus channel type (objective 1)

There are systematic variations of width, depth, velocity and friction factor with discharge in each of the study reaches, but the similarities and differences between reaches could not be easily delineated by gross morphology. The first hypothesis was based on the understanding that sources of flow resistance, which presumably influences width, depth, and velocity, may vary based on the channel type (Richards, 1976). Cascade reaches generally have steeper gradients and the major source of resistance is large boulders protruding in the flow. The resistance is mainly related to skin friction and form drag around large boulders. The major source of roughness in a step-pool reach is from energy dissipation as flow tumbles over each step and enters into the pool (Wilcox and Wohl, 2006; Curran and Wohl, 2003; Chin, 1989, 2003; Chanson, 1996; Abrahams *et al.*, 1995). Wood is a major component of resistance in both channel types, with the greatest amount being found incorporated into the steps (Figure 9). We hypothesized that these various sources of resistance would contribute to differences in the rates of change of velocity, width and depth in each of the channel reaches, but there was not a significant difference in the response between channel types.

AHG and flow resistance (objective 2)

The second hypothesis tests what specific control variables are most influential on the rates of change of width, depth and velocity with discharge. The rapid decrease in the friction factor in each reach is accommodated by an increase in both velocity and depth, with only a small change in width. Therefore, the first part of this hypothesis explores what types of flow resistance control the changes in the AHG exponents. The sources of flow resistance were represented by roughness-area, wood load, coefficient of variation of pool volume, sediment sorting (σ), sediment size (D_{84}), standard deviation of bed elevation and width/depth ratio. Both *f* and *m* are expected to be dependent on flow resistance characteristics, whereas *b* is dependent on channel shape (Ferguson, 1986; Bathurst, 1993). The only resistance characteristic that was significantly related to the PCA Axis 1 scores was the average roughness-area. The roughness-area can include both boulders and logs that make up part of the bed as well as portions of the overhanging bank that become submerged as flow increases.

It is expected that smaller roughness elements would become submerged at higher flows, allowing a marked decrease in resistance and a much higher velocity (Knighton, 1975). At lower flows water is both forced around boulders where form drag is high and over smaller submerged cobbles and pebbles. The flow resistance related to these smaller

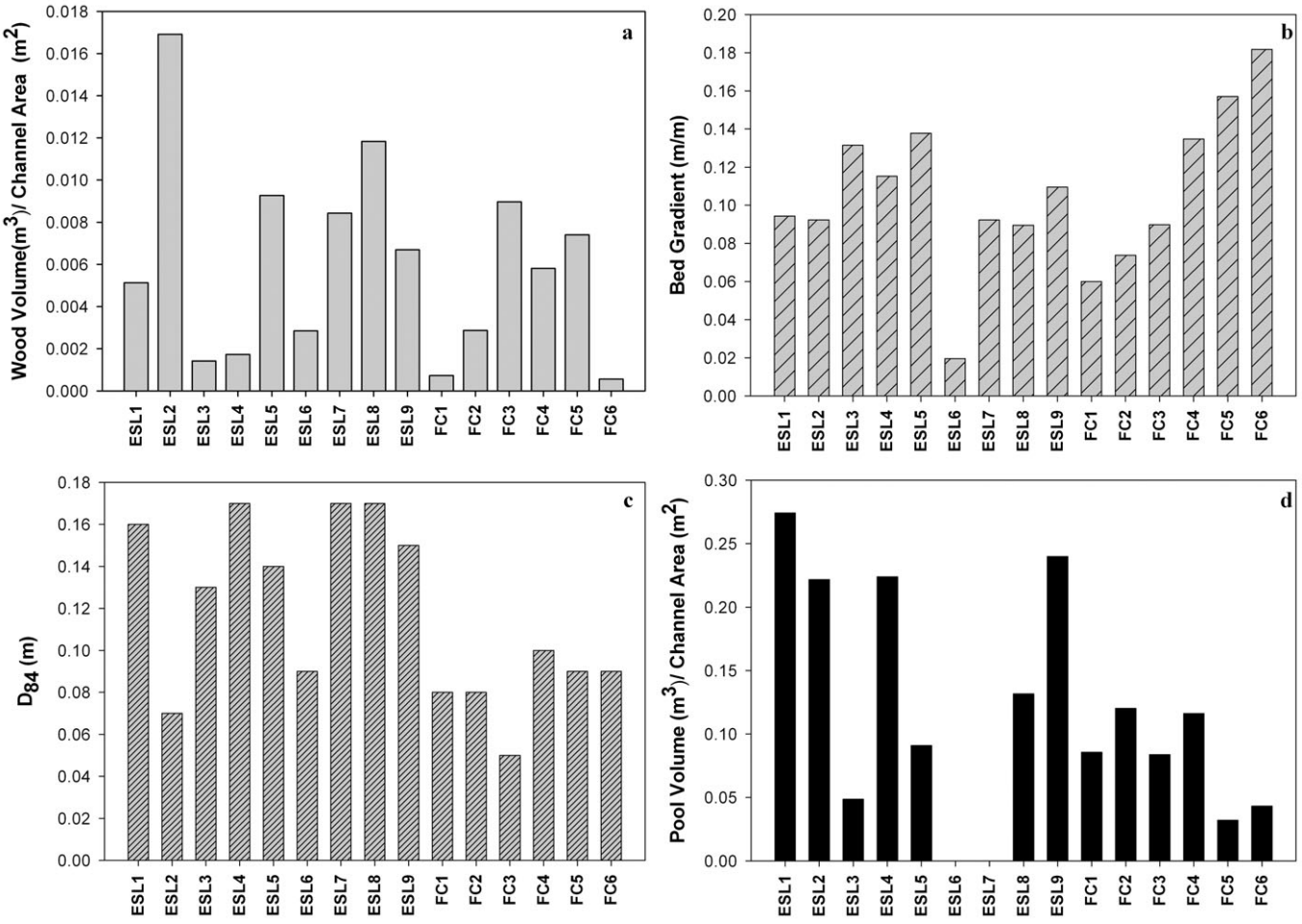

Figure 9. Barplots showing values for each reach of (a) wood volume per channel area, (b) bed gradient, (c) D_{84} and (d) pool volume per channel area.

Table IV. Correlation matrix showing correlations among four variables: D_{84}, wood volume per channel area, pool volume per channel area, and gradient

	D_{84} (m)	Wood volume per channel area (m^3/m^2)	Pool volume per channel area (m^3/m^2)	Gradient (m/m)
D_{84} (m)	–	0·00	0·30	0·12
Wood volume per channel area (m^3/m^2)	0·00	–	0·24	–0·04
Pool volume per channel area (m^3/m^2)	0·30	0·24	–	–0·03
Gradient (m/m)	0·12	–0·04	–0·03	–

grains between boulders may become increasingly significant as stage decreases (David, 2010). As discharge increases the boulders become submerged and form drag decreases and mean velocity will increase rapidly (Bathurst, 1993). Skimming flows may eventually develop over the tops of boulders at the higher stages. If the boulders are an equivalent height as the flow at all flows, then they are never submerged and form drag will remain dominant in that reach. This is why D_{84} and R/D_{84} are commonly found to be good representations of roughness in a reach (Bathurst, 1993). David *et al.* (2010) found that R/D_{84} was significantly related to friction factor in cascade reaches, but that R/H was significantly related to friction factor in step-pool reaches. Despite these distinct differences in the types of flow resistance between channel types, the AHG exponents appear to be controlled by the area of material that projects into the flow. Lee and Ferguson (2002) found that the velocity exponent (m) was related to the proportion of bankfull width that is occupied by protruding clasts at low flow. Areas with protruding clasts cause the flow field to separate and wake turbulence to increase. Table III shows that m is smaller in reaches with a larger range of clast sizes, further supporting the interpretation that larger grains have a significant effect on AHG exponents.

Sediment size and sediment sorting can play a role in influencing the velocity profile (Wiberg and Smith, 1991), but in these streams neither was found to be significantly related to the hydraulic exponents represented by the PCA Axis 1 scores. Ferguson (1986) showed theoretically that hydraulic geometry should vary with bed particle size, but Ridenour and Giardino (1995) found no correlation between median grain-size and hydraulic geometry for pool-riffle channels. The results of this study agree with Ridenour and Giardino (1995), with no significant relationship between the PCA Axis 1 scores and D_{84} or sediment sorting for cascade and step-pool channels.

There are six reaches that have high friction exponents and have velocity exponents (m) greater than $b + f$. Knighton (1975) found that the highest rates of decrease in resistance were related to cross-sections where grain resistance domi-

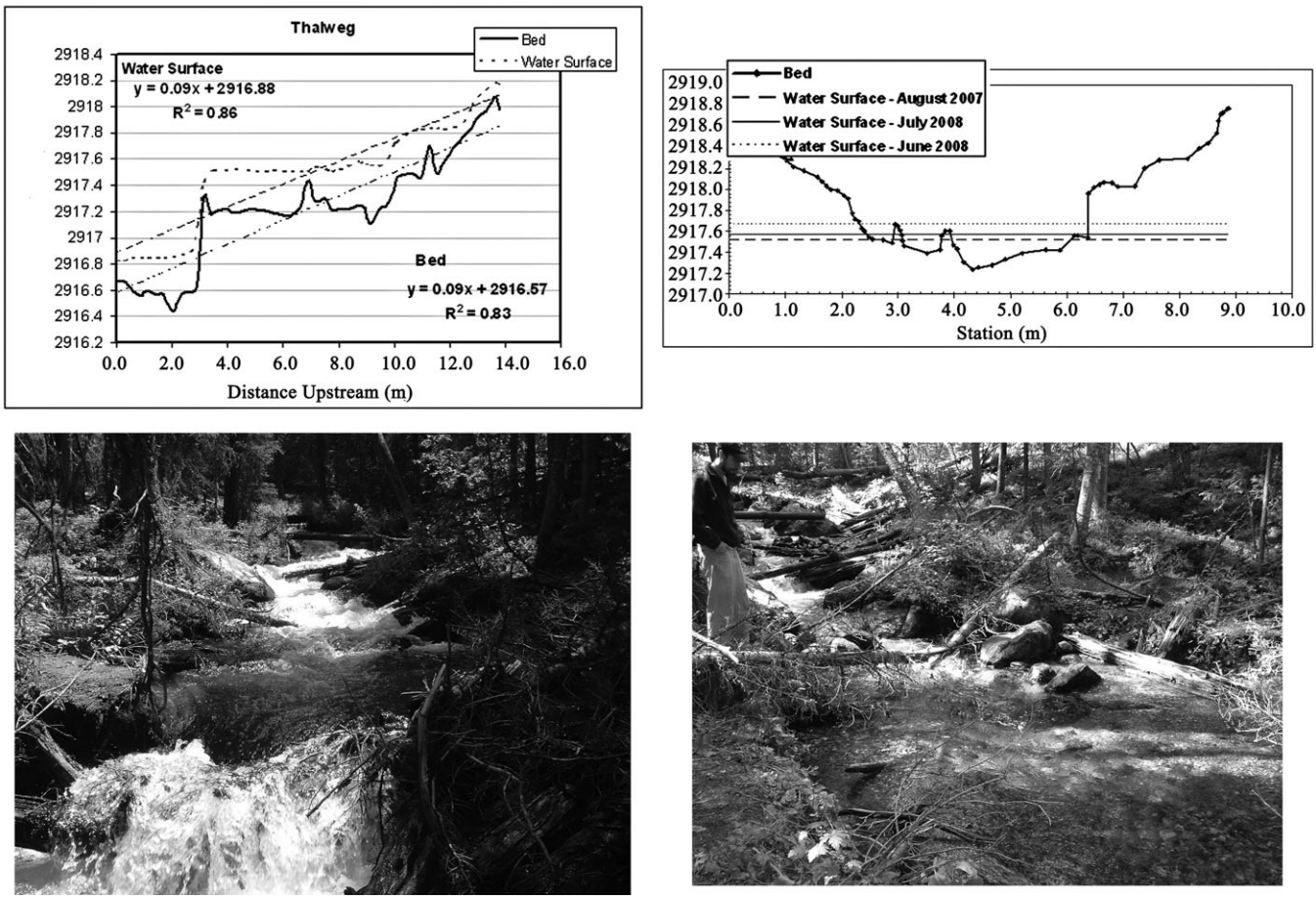

Figure 10. Example of longitudinal profile and cross-section of ESL2. The longitudinal profile shows both the bed profile and water surface with fitted linear trend lines and equations shown for both. The photograph in the bottom left shows the entire reach, looking upstream during the June 2008 high flow. The cross-section shows the water-surface elevation at three stages (August 2007, July 2008 and June 2008). The photograph on the bottom right shows the approximate location of the cross-section at August 2007 low flow.

nated. Therefore, grain resistance is probably the dominant form of resistance in these six reaches in relation to the rate of change of width, depth and velocity with discharge. Three of these are step-pool reaches (ESL2, FC1, FC4), but the results indicate that these are still highly influenced by grain resistance (Knighton, 1975). All the reaches are at different gradients, but have similar values of D_{84}. ESL2 has localized sections of very shallow gradients behind the large log step in the reach (Figure 10). The high wood load is related to this large log step, which is probably the cause for the local reduction in gradient and deposition of fine sediment (Buffington and Montgomery, 1999). The log step most likely increases the total friction in the reach, but is never completely submerged, so friction factor will remain relatively high in this reach because of the log step. However, the finer sediments behind the step are quickly submerged at high flows, meaning that the friction factor quickly decreases in this section of the reach. Therefore, the values of the exponents are influenced mainly by the grain size and not step size. FC1 and FC4 are both step-pool reaches as well, but they both are narrow reaches with local reductions in gradient and grain size that are quickly submerged as discharge increases. FC5 and FC6 are both narrow, somewhat rectangular cascade reaches (Figure 11). The high wood load in FC5 is related to one log that is embedded in the channel bottom and creates one large step in the reach. Again, the resistance related to this step remains high as discharge increases, since it is not submerged at the higher flows. As flow increases in both reaches the larger clasts are quickly submerged, allowing velocity to increase and resistance related to grains to decrease quickly with discharge. Figure 11 shows how quickly the flow submerges the roughness elements in the flow for these two reaches versus ESL7.

ESL6 is the last reach in this category. The plane-bed reach is already expected to be dominated by grain resistance, although plane-bed reaches from Reid's (2005) study did not necessarily plot in the same part of the ternary diagram. The reaches in Reid's (2005) study had had some 'previous modification', which may be why there was so much variability in this channel type.

The relative submergence (R/D_{84}) has been shown to be an important representation of grain resistance, particularly in pool-riffle channels and boulder bed streams with gradients <4% (Bathurst, 1993, 2002; Reid and Hickin, 2008). The average relative submergence was not found to be significantly related to the PCA axis scores, but Figure 8(b) shows the complexity of the relationship between R/D_{84} and the axis scores. Except for ESL1, there is a division between the FC reaches and the ESL reaches around a value of 0·3. The axis scores of ESL reaches increase with increasing CV of R/D_{84} and the FC axis scores decrease. The differences here may represent a difference in both channel shape and resistance in the FC reaches.

Other studies have also found that roughness elements such as median grain-size and drag resistance were not significantly related to the hydraulic exponents (Ridenour and Giardino, 1995). Ridenour and Giardino (1995) concluded that although roughness elements are related to velocity and depth, this does

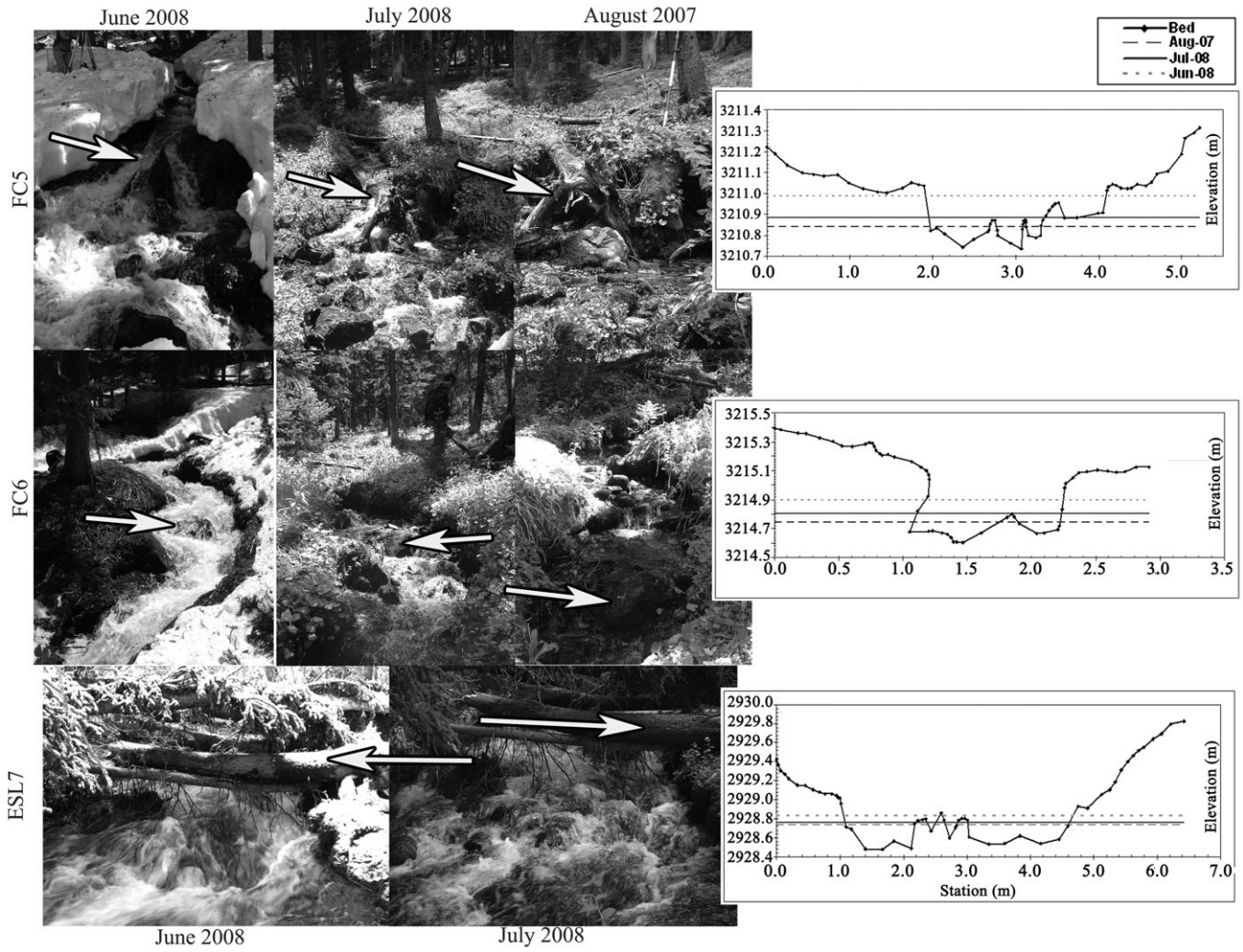

Figure 11. Photographs and cross-sections for three cascade reaches: FC5, FC6 and ESL7. The white arrows show the same location in each photograph and the photographs are of the approximate location of each of the cross-sections shown at the right. The cross-sections show the water-surface elevation over three flow periods (August 2007, July 2008 and June 2008). The photographs show those three flow periods for FC5 and FC6, but only July 2008 and June 2008 for ESL7. The same location on the reach was not photographed in August 2007.

not mean that the rates of change of velocity and depth with discharge are related to these same roughness elements (Ridenour and Giardino, 1995). Alternatively, the rates of change of velocity and depth were found to be significantly related to the rate of change of the friction factor (Figure 7) (Richards, 1973; Ridenour and Giardino, 1995). The results of this study indicate that m is negatively correlated with x. Again, the reaches that are probably dominated by changes in grain resistance have the highest values of x (Knighton, 1975). Reaches that have boulders or logs the same order of magnitude as the flow depth do not have as high a rate of change in resistance or velocity with depth. Reaches that plot in different locations on the ternary diagram may need to be evaluated separately in terms of controls on the hydraulic exponents. The small sample size in this study did not allow for development of separate multiple regressions for these reaches.

The wood volume per squared meter of channel was used to determine whether there was a significant relationship between wood and the at-a-station hydraulic exponents, but no significant relationship was found (Table III). The lack of significance in the regression could be either related to the complexity of the relationship or to the fact that, although wood is probably related to velocity in the reach, it is not necessarily related to the rate of change of velocity (Ridenour and Giardino, 1995).

Variability in the value of the exponents appears to decrease with increasing wood load (Figure 8d). This suggests that when there is a smaller amount of wood in the reach the exponent values vary more, but at higher roughness the rates of change of velocity and depth with discharge may be limited. We expect that wood would reduce the average velocity and locally elevate the water surface, but the interaction between wood, other roughness elements such as boulders, and the hydraulic exponents is probably very complex. Wilcox and Wohl (2006) found that interactions between steps, grains and wood have a significant effect on how resistance varies with discharge in step-pool streams, so we expect that the same interactions influence how velocity and depth vary with discharge in these same streams.

The friction exponent (x) was not significantly related to the wood load (Table III). The lack of a relationship is probably because the individual pieces of wood need to be categorized differently. Wilcox and Wohl (2006) found that the position of wood in the channel can have a greater effect on resistance than the density. Wood located at step lips increased the height of the step and dammed the flow. Another important characteristic is the size of the wood piece relative to water

depth (Gippel *et al.*, 1996). The resistance may not change around a large log that is submerged at all flows, but as a smaller log becomes submerged it may cause a change in resistance as flow increases. Also, a log that was not within the water column at low flow may change the resistance characteristics as it becomes submerged at higher flows. Hygelund and Manga (2003) found that drag did not vary with depth around logs that had diameters greater than one-third the channel depth. Therefore, large individual pieces in the flow would not have a large effect on how friction and velocity change with discharge. Reaches that had large single pieces of wood in the flow include ESL5, ESL9, FC1 and FC5. FC1 and FC5 both have one large log in the flow, which probably does not cause a significant difference in drag between low and high flows.

ESL5 and ESL9 both have larger log jams associated with large steps in the reach, which were expected to be a significant control on the AHG. The reaches with the largest and most complex jams are ESL1, ESL2, ESL5 and FC3. Manners *et al.* (2007) found that the frontal area and surface area of a jam have an important effect on the amount of drag related to the jam. In ESL2 the jam created a reduced water-surface slope, causing a reduction in velocity and textural fining (Figure 10). The velocity increases at one of the faster rates in ESL2 (m = 0·56) because as discharge increases these finer sediments are quickly submerged, reducing friction and increasing velocity. This is also related to the smaller rate of change of depth (f = 0·29). As the roughness elements become increasingly submerged, the water can pass through more quickly and the depth does not change as much with discharge. FC3 is slightly different because a larger portion of the reach is below the large log jam and more steps developed from other log jams. The influence of wood and sediment sorting on the at-a-station exponents may be better understood by differentiating the reaches that are dominated by the variation in grain resistance in the reach (Figure 12).

Wood, R/D_{84}, bed material size distribution, CVPoolV and average roughness-area are all variables that represent roughness in each reach from clasts, wood and bedforms. Average roughness-area is a variable that integrates grain and form roughness, which is probably why it is the variable significant in the regression with the PCA Axis 1 scores.

AHG versus gradient (objective 2)

The second significant variable in the multiple regression with the PCA Axis 1 scores is gradient (Table III). Gradient partly governs the amount of energy available for transporting material or eroding the bed and banks of a channel. Although the gradient is interrelated with each of the hydraulic variables, the bed gradient did not change significantly over the course of the study and therefore is considered as a potential control variable. Previous studies have shown the importance of gradient in controlling how resistance varies with discharge throughout a channel network (Bathurst, 1993; Comiti *et al.*, 2007; David *et al.*, 2010). As gradient increases along Axis 1, m and f increase. Therefore, as the bed steepens the rate of change of velocity and depth with discharge increases. Leopold and Maddock (1953) also found in their original hydraulic geometry study that the rates of change of width, depth and velocity are controlled by the slope of the water surface. Wohl (2007) determined that an inflection point in the rate of change of the water-surface gradient with discharge indicated the point between where grain resistance and form resistance dominated. The low sample size for each reach made it impossible to determine if inflection points exist for these reaches.

Problems with using reach-averaged hydraulic geometry

This study used reach-averaged values of width, depth and velocity to compare AHG. The use of reach-averaged values meant that the exponents did not always sum to unity for every reach. Stewardson (2005) proposed using the coefficient of variation of the width, depth and velocity to characterize the cross-sectional hydraulic geometry of a river reach, but these relations were not found to be significantly related to discharge. The use of reach-averaged values may reduce the variability in the hydraulic exponents (Jowett, 1998; Lamouroux and Capra, 2002; Stewardson, 2005), but the use of the coefficient of variation of these exponents may not be practicable for these steeper streams. It is also possible that there was a lack of relationship because the study was only done over four

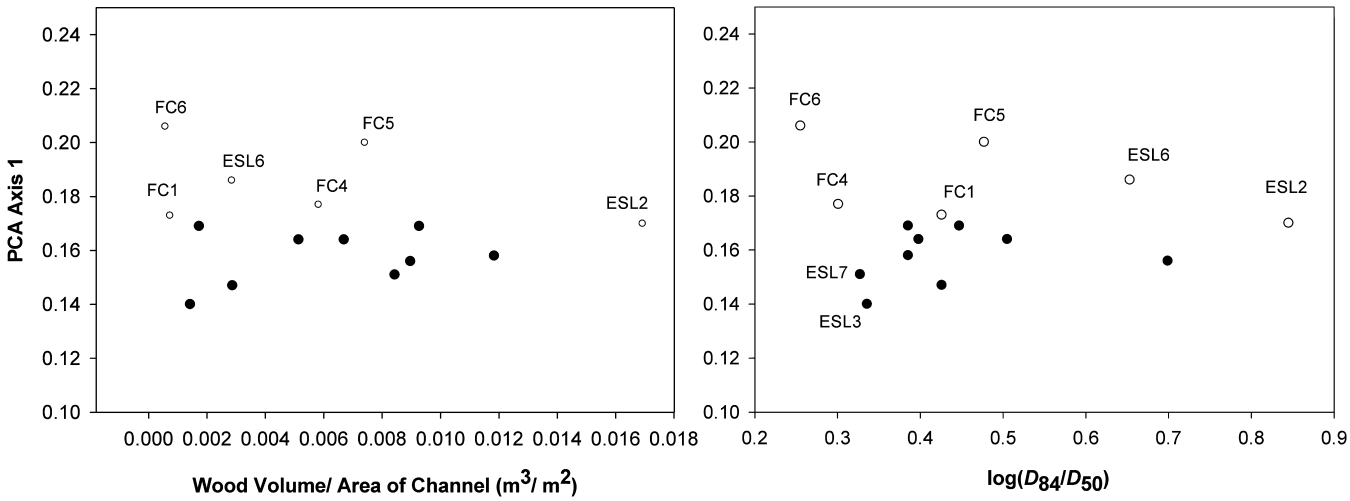

Figure 12. PCA Axis 1 scores versus wood volume per channel area (left) and log (D_{84}/D_{50}) (right). The reaches are divided by those interpreted to be dominated by grain resistance (open circles) and those that are dominated by form and spill resistance (closed circles).

flow periods. There is high variability between cross-sections in each of these reaches, but the good fit between width, depth and velocity with discharge is thought to show how well these power relations still characterize these reaches.

Conclusion

AHG is an important tool to use to help in our understanding of resistance in steep mountain streams. The hydraulic exponents at the ESL and FC sites were all within the range of values found by other researchers studying step-pool, cascade and plane-bed reaches. The exponents could not be used to delineate a difference between the three channel types, but may be useful in determining which reaches are dominated by grain resistance versus form resistance.

For most study reaches, $m > f > b$, indicating that the rate of change of velocity with discharge is greater than the rate of change of width or depth. This reflects the fact that increasing discharge in these steep, laterally confined streams results mainly in reduced effective hydraulic resistance as sources of grain and form roughness occupy a progressively smaller portion of the flow. Average exponent values for low gradient streams indicate that a larger proportion of the change in discharge is compensated by increasing flow width ($b = 0{\cdot}4$–$0{\cdot}5$), with lower rates of change in depth and velocity (Park, 1977). In contrast, increasing flow in steep mountain streams primarily alters the effective hydraulic resistance, as reflected in rates of change of velocity and flow depth. These effects increase with gradient, as reflected in higher m and f values at steeper slopes for the ESL and FC reaches.

These relations are illuminated by PCA analysis. The at-a-station values are significantly related to average roughness-area and the bed gradient in each reach. Localized reductions in gradient, sediment size and channel shape explain the connections between cascade and step-pool reaches in two basins with high values of m and x. A larger sample of the population should be tested to investigate if similar conclusions can be applied to the larger population of step-pool and cascade streams throughout the world. Reaches with $m > f + b$ have much more drastic changes in grain resistance with discharge, therefore making grain resistance the controlling resistance versus form or spill. Further work needs to be done to understand whether reaches with $m > f + b$ are all dominated by grain resistance and whether controls in these reaches should be evaluated separately from controls in reaches that may be dominated by form resistance, but our results suggest that such reaches are dominated by grain resistance and that they form one population, with respect to AHG, with reaches dominated by form resistance.

Acknowledgments—This research was funded by the Hydrologic Sciences Program of the National Science Foundation (EAR 0608918). The USDA Forest Service Rocky Mountain Research Station and field assistants Mark Hussey, Dan Dolan, Alexandra David, Lina Polvi and Dan Cadol provided logistical support. The comments of two anonymous reviewers helped us to improve this paper.

References

Abrahams AD, Li G, Atkinson JF. 1995. Step-pool streams: adjustment to maximum flow resistance. *Water Resources Research* **31**: 2593–2602.

Bates BC. 1990. A statistical log piecewise linear model of at-a-station hydraulic geometry. *Water Resources Research* **26**: 109–118.

Bathurst JC. 1982. Flow resistance in boulder-bed streams. In *Gravel-bed Rivers: Fluvial Processes, Engineering and Management*, Hey RD, Bathurst JC, Thorne CR (eds). John Wiley & Sons: Chichester; 443–465.

Bathurst JC. 1985. Flow resistance estimation in mountain rivers. *Journal of Hydraulic Engineering* **111**: 625–643.

Bathurst JC. 1993. Flow resistance through the channel network. In *Channel Network Hydrology*, Beven K, Kirkby MJ (eds). John Wiley & Sons: Chichester; 69–98.

Bathurst JC. 2002. At-a-site variation and minimum flow resistance for mountain rivers. *Journal of Hydrology* **269**: 11–26.

Buffington JM, Montgomery DR. 1999. Effects of hydraulic roughness on surface textures of gravel-bed rivers. *Water Resources Research* **35**: 3507–3521.

Chang HH. 1980. Geometry of gravel streams. *Journal of Hydraulics Division American Society of Civil Engineers* **106**(HY9): 1143–1156.

Chanson H. 1994. Comparison of energy dissipation between nappe and skimming flow regimes on stepped chutes. *Journal of Hydraulic Research* **32**: 213–219.

Chanson H. 1996. Comment on 'Step-pool streams: adjustment to maximum flow resistance' by Athol D. Abrahams, Gang Li, and Joseph F. Atkinson. *Water Resources Research* **32**: 3401–3402.

Chin A. 1989. Step-pools in stream channels. *Progress in Physical Geography* **13**: 391–408.

Chin A. 2003. The geomorphic significance of step-pools in mountain streams. *Geomorphology* **55**: 125–137.

Church M, Zimmerman A. 2007. Form and stability of step-pool channels: research progress. *Water Resources Research* **43**: W03415. DOI. 10.1029/2006WR005037

Comiti F, Mao L, Wilcox A, Wohl EE, Mario LA. 2007. Field-derived relationships for flow velocity and resistance in high-gradient streams. *Journal of Hydrology* **340**: 48–62. DOI. 10.1016/j.jhydrol.2007.03.021

Curran JH, Wohl EE. 2003. Large woody debris and flow resistance in step-pool channels, Cascade Range, Washington. *Geomorphology* **51**: 141–157.

David GCL. 2010. *Characterizing flow resistance in steep mountain streams, Fraser Experimental Forest, Colorado*, PhD Dissertation, Fort Collins, CO.

David GCL, Wohl EE, Yochum SE, Bledsoe BP. 2010. Controls on spatial variations in flow resistance along steep mountain streams. *Water Resources Research*. **46**: W03513. DOI. 10.1029/2009WR008134

Ferguson RI. 1986. Hydraulics and hydraulic geometry. *Progress in Physical Geography* **10**: 1–31.

Ferguson RI. 2007. Flow resistance equations for gravel- and boulder-bed streams, Water Resources Research 43: W05427.DOI:10.1029/2006WR005422.

Gippel CJ, Finlayson BL, O'Neill IC. 1996. Distribution and hydraulic significance of large woody debris in lowland Australian river. *Hydrobiologia* **318**: 179–194.

Grant GE, Swanson FJ, Wolman MG. 1990. Pattern and origin of stepped-bed morphology in high-gradient streams, Western Cascades, Oregon. *Geological Society of American Bulletin* **102**: 340–352.

Hickin EJ. 1995. Hydraulic geometry and channel scour, Fraser River, British Columbia, Canada. In *River Geomorphology*, Hickin EJ (ed.). John Wiley & Sons: Chichester; 155–167.

Hogan DL, Church M. 1989. Hydraulic geometry in small, coastal streams – progress toward quantification of salmonid habitat. *Canadian Journal of Fisheries and Aquatic Sciences* **46**: 844–852.

Huang HQ, Nanson GC. 2000. Hydraulic geometry and maximum flow efficiency as products of the principle of least action. *Earth Surface Processes and Landforms* **25**: 1–16.

Hygelund B, Manga M. 2003. Field measurements of drag coefficients for model large woody debris. *Geomorphology* **51**: 175–185.

Jarrett RD. 1984. Hydraulics of high-gradient streams. *Journal of Hydraulic Engineering* **110**: 1519–1539.

Jowett IG. 1998. Hydraulic geometry of New Zealand rivers and its use as a preliminary method of habitat assessment. *Regulated Rivers: Research and Management* **14**: 451–466.

Kirkby MJ. 1977. Maximum sediment efficiency as a criterion for alluvial channels. In *River Channel Changes*, Gregory KJ (ed.). Wiley-Interscience: Chichester; 429–442.

Knighton AD. 1974. Variation in width-discharge relation and some implications for hydraulic geometry. *Geological Society of America Bulletin* **85**: 1069–1076.

Knighton AD. 1975. Variations in at-a-station hydraulic geometry. *American Journal of Science* **275**: 186–218.

Knighton AD. 1998. *Fluvial Forms and Processes*. Oxford University Press: New York.

Kovach Computing System. 2002. *Multivariate Statistical Package (MVSP)*. Kovach Computing: Anglesey.

Kutner MH, Nachtsheim CJ, Neter J, Li W. 2005. *Applied Linear Statistical Models*. McGraw-Hill/Irwin: New York; 1396 pp.

Lamouroux N, Capra H. 2002. Simple predictions of instream habitat model outputs for target fish populations. *Freshwater Biology* **47**: 1543–1556.

Langbein WB. 1964. Geometry of river channels. *Journal of Hydraulic Division, Proceedings of the American Society of Civil Engineers* **90**: 301–312.

Lawrence D. 2007. Analytical derivation of at-a-station hydraulic geometry relations. *Journal of Hydrology* **334**: 17–27.

Lee AJ, Ferguson RI. 2002. Velocity and flow resistance in step-pool streams. *Geomorphology* **46**: 59–71.

Leica Geosystems. 2008. *Cyclone 5.8.1.*: *Comprehensive Software for Working with Laser Scan Data*. Leica Geosystems HDS LLC: San Ramon, CA.

Leopold LB, Maddock T. 1953. The hydraulic geometry of stream channels and some physiographic implications. *US Geological Survey Professional Paper* **252**: 57 pp.

Leopold LB, Bagnold RA, Wolman MG, Brush LM. 1960. Flow resistance in sinuous or irregular channels. *US Geological Survey Professional Papers* **282D**: 111–134.

Manga M, Kirchner JW. 2000. Stress partitioning in streams by large woody debris. *Water Resources Research* **36**: 2373–2379.

Manners RB, Doyle MW, Small MJ. 2007. Structure and hydraulics of natural woody debris jams. *Water Resources Research* **43**: W06432. DOI. 10.1029/2006WR004910

McCune B, Grace JB. 2002. *Analysis of Ecological Communities*. MjM Software Design: Gleneden Beach, OR; 300 pp.

Montgomery DR, Buffington JM. 1997. Channel-reach morphology in mountain drainage basins. *Geological Society of America Bulletin* **109**: 596–611.

Park CC. 1977. World-wide variations in hydraulic geometry exponents of stream channels: an analysis and some observations. *Journal of Hydrology* **33**: 133–146.

Phillips JD. 1990. The instability of hydraulic geometry. *Water Resources Research* **26**: 739–744.

R Core Development Team. 2007. *R: A Language and Environment for Statistical Computing*. R Foundation for Statistical Computing: Vienna.

Reid DE. 2005. *Low-flow Hydraulic Geometry of Small Steep Streams in Southwest British Columbia*, MSc Thesis, Simon Fraser University.

Reid DE, Hickin EJ. 2008. Flow resistance in steep mountain streams. *Earth Surface Processes and Landforms* **33**: 2211–2240. DOI. 10.1002/esp.1682.

Rhoads BL. 1992. Statistical models of fluvial systems. *Geomorphology* **5**: 433–455.

Rhodes DD. 1977. The b-f-m diagram: graphical representation and interpretation of at-a-station hydraulic geometry. *American Journal of Science* **277**: 73–96.

Richards KS. 1973. Hydraulic geometry and channel roughness – a non-linear system. *American Journal of Science* **273**: 877–896.

Richards KS. 1976. Complex width-discharge relations in natural river sections. *Geological Society of America Bulletin* **87**: 199–206.

Ridenour GS, Giardino JR. 1991. The statistical study of hydraulic geometry: a new direction for compositional data analysis. *Mathematical Geology* **23**: 349–366.

Ridenour GS, Giardino JR. 1995. Logratio linear modeling of hydraulic geometry using indices of flow resistance as covariates. *Geomorphology* **14**: 65–72.

Singh VP, Zhang L. 2008a. At-a-station hydraulic geometry relations, 1: theoretical development. *Hydrological Processes* **22**: 189–215. DOI. 10.1002/hyp.6411

Singh VP, Zhang L. 2008b. At-a-station hydraulic geometry relations, 2: calibration and testing. *Hydrological Processes* **22**: 216–228. DOI. 10.1002/hyp.6412

Stewardson M. 2005. Hydraulic geometry of stream reaches. *Journal of Hydrology* **206**: 97–111. DOI. 10.1016/j.jydrol.2004.09.004

Taylor RB. 1975. *Geologic Map of the Bottle Pass Quadrangle, Grand County, Colorado*. Cr.S. Geological Survey map GQ-1244. Scale 1:24,000.

Trayler CR, Wohl EE. 2000. Seasonal changes in bed elevation in a step-pool channel, Rocky Mountains, Colorado, U.S.A. *Arctic, Antarctic, and Alpine Research* **32**: 95–103.

USDA Forest Service. 2009. *About Fraser Experimental Forest*. http://www.fs.fed.us/rm/fraser/about/index.shtml.

White WR, Bettess R, Paris E. 1982. Analytical approach to river regime. *Journal of the Hydraulics Division American Society of Civil Engineers* **108**: 1179–1193.

Wiberg PL, Smith JD. 1991. Velocity distribution and bed roughness in high-gradient streams. *Water Resources Research* **27**: 825–838.

Wilcox AC, Wohl EE. 2006. Flow resistance dynamics in step-pool stream channels: 1. Large woody debris and controls on total resistance. *Water Resources Research* **42**: W05418. DOI. 10.1029/2005WR004277

Wohl E. 2007. Channel-unit hydraulics on a pool-riffle channel. *Physical Geography* **28**: 233–248.

Wohl E, Kuzma JN, Brown NE. 2004. Reach-scale channel geometry of a mountain river. *Earth Surface Processes and Landforms* **29**: 969–981. DOI. 10.1002/esp.1078

Wolman MG. 1954. A method for sampling coarse river-bed material. *Transactions-American Geophysical Union* **35**: 951–956.

Yang CT. 1976. Minimum unit stream power and fluvial hydraulics. *Journal of the Hydraulics Division American Civil Engineers* **102**(HY7): 919–934.